Universality of properties of coil–globule transitions in different two-dimensional lattice models of a macromolecule

T. M. Birshtein and S. V. Buldyrev*
Institute of High Molecular Compounds of the Academy of Sciences of the USSR, Bolshoy Prospect 31, St Petersburg, USSR
(Received 24 January 1990; revised 29 June 1990; accepted 3 July 1990)

Using a Monte-Carlo method, we study the behaviour of different lattice models of a linear macromolecule in the θ-point region. Paying most attention to the testing of new theoretical concepts of the two-dimensional θ point[1,2], we give a new interpretation of some numerical results of our previous work[3,4] and generalize others. We confirm the assumption of the universality of the value of the tricritical exponent $\nu_t = 4/7$. The values of ν_t for a self-avoiding walk (SAW) on triangular, square and honeycomb lattices as well as for two special models, viz. infinitely prolonging self-avoiding walks (IPSAW)[3] and infinitely growing self-avoiding walks with nearest-neighbour interactions (IGSAWN)[5], lie between 0.56 and 0.59. The slight differences between these results can be explained by the effect of the corrections to scaling, which have different values for different models. The values of the crossover exponent φ_t are confined between 0.42 and 0.6, which is not in complete contradiction with the value $\varphi_t = 3/7$ for the θ point, proposed elsewhere[2], but differ from our previous result $\varphi_t = 0.6 \pm 0.1$ obtained earlier[3,4] without extrapolation to the limit $N \to \infty$, where N is the length of a chain. The values of the free-energy exponent γ_t determined in the present work lie between 0.98 and 1.07, and, thus, do not coincide with the value of $\gamma_t = 8/7$ proposed by others[2]. The value of $\gamma_{1t} = 0.5 \pm 0.05$ that we obtained for a polymer confined in a half-space is in complete contradiction with the above result[2] for the θ point. As a whole, our results are in good agreement with recent work[6,7] using a similar technique for shorter SAWs on a square lattice.

(Keywords: polymer solution; coil–globule transition; two-dimensional lattice models; Monte-Carlo method; random-walk models; tricritical exponents; theta points; universality classes; scaling)

INTRODUCTION

In the past few years some very interesting theoretical results concerning the behaviour of a two-dimensional polymer chain near the θ point have been obtained[1,2]. However, the problem of the universality of the two-dimensional θ point is still rather ambiguous[8–11]. De Gennes in 1975 was the first to describe the θ point as a tricritical point[12]. In the three-dimensional case ($d=3$) the question about the values of tricritical exponents appeared to be rather simple because $d=3$ is the upper critical dimension for the three-body interactions and, therefore, the values of tricritical exponents are Gaussian: $\nu_t = \varphi_t = 1/2$, $\gamma_t = 1$. In the two-dimensional case ($d=2$) this question is still open. The discussion on the values of the tricritical exponents in two dimensions was initiated by the work of de Gennes[12], where the mean-field values $\nu_t = 2/3$, $\varphi_t = 1/3$ as well as the field-theory values $\nu_t = 0.505$, $\varphi_t = 0.64$ were proposed. The latter were obtained by means of the ε-expansion method in powers of $\varepsilon = 3 - d$ for the model $\varphi^4 + \varphi^6$ ($\varphi \in R^n$) in the limit $n \to 0$. It should be mentioned that, for the ordinary critical point of the φ^4 model in the limit $n \to 0$, characterizing the behaviour of a long polymer in a good solvent, both mean-field and ε-expansion methods give[13] very close values for the critical exponent ν. Moreover, in the two-dimensional case the mean-field value $\nu = 3/4$ coincides with the exact value, obtained by Nienhuis[14] by means of the Coulomb gas model. Such a huge discrepancy between the predictions of these two methods for the tricritical exponents in two dimensions aroused numerous theoretical, numerical and experimental attempts to determine their true value[15–44]. For a long time, however, these attempts did not lead to any reliable result. Eventually, in 1985, a number of works appeared simultaneously, in which intermediate values of the exponent ν_t close to $4/7 \simeq 0.57$ were obtained independently and by different methods[3,5,24,38].

The most interesting one of these was the work of Weinrib and Trugman[24], who introduced a new type of random walk, called a smart kinetic walk (SKW). On the one hand, this walk can be considered as a model of a polymer ring on a honeycomb lattice, with the interaction of all nearest-neighbour (NN) and some next-nearest-neighbour (NNN) monomers. On the other hand, it can be considered as the external perimeter (hull) of a cluster on the dual triangular lattice at the percolation threshold. The fractal dimension of the hull, d_h, as has now been strictly established[45], is equal to 7/4. As was generally acknowledged, a polymer with local monomer interaction of any type has to belong to one of three universality classes: (i) the class of good solvents in which the dependence of the mean size D of a macromolecule *versus* its number of links N is described by the asymptote:

$$D \sim N^{\nu} \qquad (\nu = 3/4) \tag{1}$$

(ii) the class of poor solvents in which:

$$D \sim N^{1/d} \qquad (d=2) \tag{2}$$

* Present address: Center for Polymer Studies, Department of Physics, Boston University, Commonwealth Avenue, Boston, MA 02215, USA

0032-3861/91/183387-21

Table 1 The values of tricritical exponents, according to different literature sources

Theory, method	Year	Ref.	ν_t	φ_t	γ_t
ε-expansion	1975	12,15	0.5055	0.6364	1.0103
	1984	16[a]	0.55	0.8	1.01
	1986	17,18	0.5055	0.6364	1.01
Mean-field theory of Flory's type[b]	1975	12,19	2/3	1/3	–
Mean-field theory of globulae–coil transition	1980	23	3/4	1/2	–
Theory of percolation	1985	24	0.57	–	–
Kinetically growing walks	1984	25	0.66	–	–
	1985	5	0.56	–	1
Concepts of universality classes	1986	26	4/7	–	–
	1987	1	4/7	–	1?
	1987	2	4/7	3/7	8/7
Theory of superconformal invariance	1988	27	4/7	3/7	15/14
Method of exact enumeration	1985	28	0.505	0.64	–
	1986	29,30	0.53	0.64	1.0
Monte-Carlo methods	1982	31	0.5055	0.64	–
	1982	32	0.66	–	–
	1985	3,4	0.59	0.6	–
	1988	33	0.58	0.6	1.0
	1988	6,7	0.57	0.52	1.1
	1988	34	0.57	0.8	1.133
	1988	35	≈ 0.5	≈ 0.5	–
Methods of real-space renormalization	1981	36	0.53	0.5	–
	1987	37	0.49	–	–
Methods of transfer matrix	1985	38	0.55	–	–
	1987	39	0.55	0.48	0.99
Method of fractal lattices	1987	40	0.546	–	–
Measurements of surface tension in real experiments	1980	41	0.56	–	–
	1985	43	0.51	–	–
	1983	42	0.51	0.64	–
	1988	44	>0.53	–	–

[a] Ref. 16 contained an error that was found later in refs. 17 and 18
[b] Flory himself found in ref. 19 only the exponents ν and ν_t in three dimensions. For the exponents ν_t and φ_t in two dimensions his method was applied in refs. 20–22.

and (iii) the class of θ solvents with asymptote:

$$D \sim N^{\nu_t} \qquad (1/d \leqslant \nu_t \leqslant \nu) \tag{3}$$

According to this idea and taking into account the value of $d_h = 7/4$ (ref. 1), one can immediately conclude that:

$$\nu_t = 1/d_h = 4/7 \tag{4}$$

Subsequently Duplantier and Saleur[2] constructed a new model of a polymer in a solvent with NN and NNN interactions. In their model, the polymer is represented by a walk on a dilute honeycomb lattice, i.e. a lattice in which some of the hexagons are forbidden for the walk with probability p, the value $p - 1/2$ corresponding to the reduced temperature $\tau \sim T - \theta$ of the system. For this model they obtained the exact values of the tricritical exponents:

$$\nu_t = 4/7 \qquad \varphi_t = 3/7 \qquad \gamma_t = 8/7 \tag{5}$$

Thus these values appeared very likely to be the exact values of the tricritical exponents characterizing the behaviour of any two-dimensional polymer near the θ point. However, this proposition is based only on the general concept of critical phenomena that the properties of a system near the critical point must not depend on the microscopic structure of the model (the geometry of local interactions, the type of lattice, and so on) and needs careful numerical and experimental testing.

Recently a proposal was put forward in some theoretical papers[8–11] that the θ point of a polymer with NN interactions only and the tricritical point of the model[2], which is called the θ' point, belong to different universality classes. However, the universality of the exponent $\nu_t = 4/7$ has been confirmed in many recent works[5,6,33–35]. The latest experimental measurements[44] of the exponent ν_t, which have established the lower boundary for its value $\nu_t \geqslant 0.53$, also do not contradict these results (cf. earlier works[41,43]).

On the contrary, the values of the exponents γ_t and φ_t appear to be non-universal, especially if one compares the value of $\gamma_t = 8/7$ (ref. 2) with the exact value $\gamma_t = 1$ for the model of an infinitely growing self-avoiding walk[5], which can also be considered as a model of a polymer under θ conditions.

In *Table 1* we summarize all known attempts to

determine the tricritical exponents of a two-dimensional polymer. The aim of the present work is to add one more line to this table. Our paper has the following structure. The Monte-Carlo technique is described first. Then we investigate the dependence of chain size on temperature and number of links in order to determine the θ temperature and the critical exponent ν_t for each model. In the following section we analyse the free energy and determine the exponent γ_t. The crossover exponent φ_t is then determined and the scaling functions are constructed. The final section contains a detailed discussion of our results and their connection with recent results of other authors. Finally, the article contains three appendices devoted to some special questions of the behaviour of random-walk models.

MONTE-CARLO SIMULATION TECHNIQUE

We study three models of a macromolecule with one lyophilic end in a solvent, which we call one-prolonging self-avoiding walks (1PSAW) on square (1PSAWS), triangular (1PSAWT) and honeycomb (1PSAWH) lattices. Besides this, we study the model of an infinitely prolonging self-avoiding walk on a square lattice (IPSAWS), corresponding to the initial parts of very long macromolecules. These initial parts, owing to self-similarity, have the same conformational characteristics as the whole chain but are more convenient for numerical study. The idea of nPSAW, where n is an arbitrary integer or infinity, appeared for the first time some while ago[46,47]. We also generalized the model of an infinitely growing self-avoiding walk on a square lattice (IGSAWS)[5], closely related to IPSAWS, introducing interaction between nearest-neighbour monomers.

The quality of solvent was simulated as usual by introducing the interaction energy $E=-\Phi kT$ (k is the Boltzmann constant, T is absolute temperature) for every pair of monomers occupying neighbouring lattice sites but not being connected by one step. We regard as monomers the lattice sites through which the walk has passed, so that a walk of N steps corresponds to a macromolecule of $N+1$ monomers and N chemical bonds. Thus, the internal energy of the ith walk containing η_i pairs of interacting monomers is equal to $-\Phi\eta_i kT$.

In each numerical experiment we constructed M statistically independent SAWs by means of the Rosenbluths' method[48] modified according to the recommendations of McCrackin[49,50], and expanded by introduction of the construction potential Ψ (ref. 3) and the topological factor t_{ijk}, which allow one to increase the importance of sampling and to moderate the attrition (the dying out) of chains as their length N is growing, respectively.

The jth ($j\geqslant 2$) step of the ith walk ($i=1,2,\ldots,M$) can be made to one of the σ_{ij} neighbouring free sites. Obviously, $0\leqslant\sigma_{ij}\leqslant z-1$, where z is the coordination number of the lattice ($z=4$ for square, $z=6$ for triangular and $z=3$ for honeycomb lattices). The probabilities p_{ijk} of transitions to these sites are not equal to each other but depend on the number η_{ijk} ($k=1,2,\ldots,\sigma_{ij}$ is the number of the site) of new contacts between the monomers that would appear if the step were made to the kth site. These probabilities are determined by the equation:

$$P_{ijk}=\rho_{ijk}\Big/\left(\sum_{k=1}^{\sigma_{ij}}\rho_{ijk}\right) \tag{6}$$

where

$$\rho_{ijk}=\exp(\Psi\eta_{ijk})t_{ijk} \tag{7}$$

where Ψ is the construction potential and t_{ijk} is the topological factor.

Varying Ψ, one can obtain with greater probability conformations of chains that have many ($\Psi>0$) or few ($\Psi<0$) monomer–monomer contacts.

In the standard SAW model $t_{ijk}\equiv 1$, but in our models t_{ijk} can be equal to zero or unity (see later), so that the number σ'_{ij} of real opportunities of making the jth step can be less than or equal to the initial number of free neighbouring sites:

$$\sigma'_{ij}=\sum_{k=1}^{\sigma_{ij}}t_{ijk}\leqslant\sigma_{ij} \tag{8}$$

When $\sigma'_{ij}=0$ the jth step of ith walk is impossible in the framework of the given model. Such a walk should be terminated and should be included in the sample of longer chains ($N\geqslant j$) with zero statistical weight.

The average value of a conformational characteristic Q is calculated according to the equations:

$$\langle Q\rangle=(1/M)\sum_{i-1}^{M}Q_i f_i/\langle Z\rangle \tag{9}$$

$$\langle Z\rangle=(1/M)\sum_{i=1}^{M}f_i \tag{10}$$

Here Q_i is the value of the conformational characteristic for the ith walk and F_i is the statistical weight of the ith walk:

$$f_i=r_i b_i w_i \tag{11}$$

where $w_i=1$ for a walk that has attained the given length N and $w_i=0$ for a walk that has been terminated at the (N_i+1)th step ($\sigma_{i,N_i+1}=0$, $N_i<N$), $b_i=\exp(\eta_i\Phi)$ is the Boltzmann factor and r_i is the Rosenbluths' factor. The latter is inversely proportional to the probability of construction of the ith walk:

$$r_i=1/p_i=1\Big/\prod_{j=1}^{N}p_{ij} \tag{12}$$

where $p_{ij}=p_{ij}k_{ij}$ is the probability of the k_{ij}th direction of the jth step that has been chosen during the construction of the ith walk. If the walk has been terminated, i.e. if $N_i<N$, the product $r_i w_i$ is put equal to zero.

It should be noted that:

$$\sum_{i=1}^{M}w_i=M(N) \tag{13}$$

where $M(N)$ is the number of walks in the given sample that have attained the length N.

Consider now how to choose the topological factor t_{ijk}. It is known that the ratio $M(N)/M$ of the number of 'survived' walks of length N to the total number of all started ones decreases exponentially when N is growing. As shown in Appendix 1, this ratio appears to

be the Monte-Carlo estimate of the partition function of the model of kinetically growing walks (KGW)[25] and must obey the equation:

$$M(N)/M \approx Z_{KGW}(N) \sim \zeta_0^N N^{\delta_{KGW}-1} \tag{14}$$

where $\zeta_0 < 1$ is some non-universal constant and $\gamma_{KGW} = \gamma = 43/32$ (ref. 14) is the critical exponent of the free energy of the standard SAW model without monomer interaction and does not depend on the type of lattice and the value of Ψ. For SAW on a square lattice ($\Psi = 0$, $t_{ijk} \equiv 1$), $\zeta_0 = 0.977$[51]. In order to increase ζ_0 and thereby to enrich the sample in long chains with the number of all started walks M being unchanged, we define t_{ijk} as:

$$t_{ijk} = \begin{cases} 0 & \eta_{ijk} = z-1 \\ 1 & \eta_{ijk} < z-1 \end{cases} \tag{15}$$

Using this rule, we obtain only such SAWs that can be prolonged at least by one step. We call this model the model of one-prolonging self-avoiding walks (1PSAW). The mathematical expectation value of the ratio $M(N)/M$ for 1PSAW has, as shown in Appendix 1, the asymptote:

$$M(N)/M \sim \zeta_1^N N^{\gamma-1} \tag{16}$$

where $\zeta_1 > \zeta_0$. The value of ζ_1 depends on z and Ψ (for $z = 4$ and $\Psi = 0$, $\zeta_1 = 0.987$). The exponent γ is universal and is equal to 43/32 as in ref 14.

Naturally, the number $L_1(N)$ of all 1PSAWs N steps long is less than the number $L(N)$ of all SAWs of the same length and satisfies the following inequality:

$$L(N) > L_1(N) > \frac{L(N+1)}{z-1} > \frac{L(N)\tilde{z}}{z-1} \tag{17}$$

where $\tilde{z}$ is the connective constant of a lattice. However, all the asymptotic properties of the 1PSAW model are the same as those of the SAW model and can differ only by the factor $(1+O(1/N))$. Besides the 1PSAW model we have also studied the model of infinitely prolonging self-avoiding walks on a square lattice (IPSAWS), which make an even smaller subset of all SAWs. In this model the factor t_{ijk} is equal to zero for all such directions of the jth step that ultimately will lead after some steps to a trap, i.e. to the impossibility of prolonging the ith walk without self-intersection. For all other directions the factor t_{ijk} is equal to unity. The algorithm for constructing IPSAWS was invented in ref. 3 and simultaneously in ref. 5, where its detailed description can be found.

The number $M(N)$ in the IPSAW model does not depend on N and is equal to the number M of all initially started walks, which is very advantageous for constructing long walks. On the contrary, the number $L_\infty(N)$ of all IPSAW of length N is less than $L(N)$, but the limit of their ratio $\lim_{N\to\infty} L_\infty(N)/L(N)$ is still unknown. The processing of data for the exact enumeration[5] gives for $L_\infty(N)$ the same parameters of the asymptote as for $L(N)$. Our numerical data also show evidence of coincidence of the universality classes of IPSAW and 1PSAW (see Appendix 2).

Besides the 1PSAW and IPSAW models we have also studied the IGSAWS model on a square lattice with interaction of nearest-neighbouring monomers ($-0.06 \leqslant \Phi \leqslant 0.06$), which differs from the IPSAWS model only in that the factor r_i in equation (11) is always equal to unity and $\Psi = 0$. Besides the models of walks on an infinite plane we also study the 1PSAWS model confined to the half-plane $x \geqslant 0$ with the origin attached to the boundary $x = 0$.

Now we shall describe how to choose the optimal value of the construction potential Ψ.

The quantity $\langle Z \rangle$ in equation (10) is an estimate of the partition function of a given model. Its variance, apparently, is M times less than the variance of f_i. But the variance of f_i is extremely large, owing to the factor r_i when Φ is close to zero and the factor b_i when Φ is large. For the classical Rosenbluths' method ($\Psi = 0$)[49] the variance of f_i attains its minimum at some value of $\Phi = \Phi_f$, when these two factors compensate each other. This value Φ_f is somewhat less than the hypothetical value Φ_θ, which corresponds to the θ point. For example, for the SAWH model ($\Psi = 0$) f_i is exactly equal to w_i when $\Phi = \ln 2$, and a non-zero variance of f_i exists at this value of parameter Φ only because some walks do not attain the given length N and their statistical weight $f_i = 0$. It should be noted that the SAWH model with $\Phi = \ln 2$ is identical to the model of kinetically growing walks (KGW) on a honeycomb lattice[25].

Varying the construction potential, we can decrease the variance of f_i for the values of Φ close to Φ_f. For each value of Φ, an optimal value of $\Psi = \Psi_{opt}(\Phi)$ exists at which the variance of f_i attains its minimum. When $\Phi < \Phi_f$, Ψ_{opt} is negative, and when $\Phi > \Phi_f$, Ψ_{opt} is positive. However, in the regions $\Phi > \Phi_\theta$ or $\Phi < 0$, we cannot obtain any considerable decrease in the variance of f_i using the construction potential.

In order to speed up the computer routine, we calculate the effective number of walks in the sample M_{eff} instead of f_i, M_{eff} is determined by the equation:

$$M_{eff} = \sum_{i=1}^{M} f_i/f_{max} \tag{18}$$

where f_{max} is the maximal value of statistical weight f_i that has occurred in these M trials. It has been established[3] that one can consider the data for a given sample as satisfactory if $M_{eff} > 100$. (For these values of M_{eff}, the coefficient of variation is less than 1%.)

When obtaining a sample of long chains (of length N_{max}) constructed with the same value of Ψ, we calculate averages at some smaller values of N ($N = N_0 + k\Delta N$, $k = 0, 1, 2, \ldots, (N_{max} - N_0)/\Delta N$) and for some values of interaction parameter Φ. At this point the Rosenbluths' method is more convenient than the method of Metropolis used elsewhere[31,32,35], where it is necessary to construct a new Markovian chain for each value of N and Φ. Naturally, the errors of the obtained data depend strongly on N and Φ. The number of walks M in different samples is a quantity of order 10^6, the length N_{max} of the walks is 150–300 steps and ΔN is equal to 10 or 20. In all samples the condition $M_{eff} > 100$ is satisfied for all values of N and in the majority of samples the condition $M_{eff} > 1000$ is satisfied for $N = 150$.

The arithmetic mean of the statistical weight f_i, giving the estimate of the partition function, and the ratio $M(N)/M$, being an estimate for the partition function of the KGW model, have been calculated in each sample. Besides these we calculate using equation (9) the following characteristics of the chain.

(i) The square of the end-to-end distance:

$$R_i^2 = x_{iN}^2 + y_{iN}^2$$

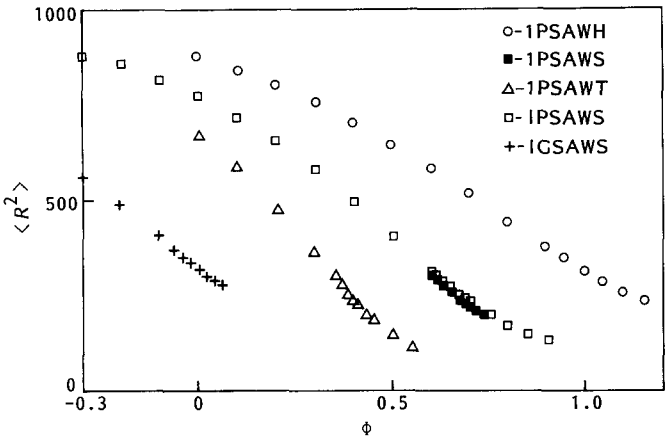

Figure 1 The dependences of $\langle R^2 \rangle$ on the interaction parameter Φ at $N=99$ for different models

where x_{ij}, y_{ij} are the coordinates of the jth monomer of the ith chain ($x_{i0}=0$, $y_{i0}=0$, $x_{i1}=1$, $y_{i1}=0$).

(ii) The square radius of gyration:

$$S_i^2=\frac{1}{N+1}\sum_{j=0}^{N}\left[\left(x_{ij}-\frac{1}{N+1}\sum_{k=0}^{N}x_{ik}\right)^2+\left(y_{ij}-\frac{1}{N+1}\sum_{k=0}^{N}y_{ij}\right)^2\right] \quad (19)$$

(iii) The number of contacts between the monomers, η_i, which is proportional to the internal energy.

(iv) The square of this number, η_i^2, which is necessary for calculation of the specific heat.

DETERMINATION OF θ POINT AND TRICRITICAL EXPONENT ν_t FROM THE DEPENDENCE OF CHAIN SIZE ON NUMBER OF LINKS

As mentioned before[3], the main problem in the analysis of the numerical data is how to determine correctly the location of the θ point, for without that, the determination of other characteristics of the transition, especially the critical exponents, cannot be carried out.

The most obvious change in the coil–globule transition is demonstrated by the mean sizes of the chain $\langle R^2 \rangle$ and $\langle S^2 \rangle$ (see *Figure 1*, which represents the dependence of $\langle R^2 \rangle$ on Φ for all models studied in the present paper). The longer the chain, the faster it grows with increase of temperature T, which can be identified in the numerical experiment with $1/\Phi$.

It is clear that the neighbourhood of the θ point must correspond to the region of the most rapid decrease of $\langle R^2 \rangle$ with increase of Φ or, in other words, the neighbourhood of the inflection point of these curves. The inflection points are located in the parameter Φ intervals (0.4, 0.5), (0.6, 0.7) and (0.9, 1.1) for the 1PSAWT, 1PSAWS and 1PSAWH models, respectively, which agrees with the θ values of parameter Φ, determined by other methods. However, this method of determination of the θ point is utterly inaccurate and may lead to erroneous results, cf. ref. 28. We developed[3] a more reliable method of simultaneous determination of the θ point and the exponent ν_t using the changes of the slope of molecular-mass dependences of chain size plotted on log–log scale at different values of parameter Φ. This method is based on the scaling theory of de Gennes[12] in which the θ point is determined as the point of change of the asymptotic regimes of molecular-mass dependences of the sizes of a macromolecular coil. The equations of that work[12] are the simplest equations that realize a smooth crossover between two regimes above and below the θ point (see equations (1)–(3)) and involve three free parameters, Φ_θ, ν_t, φ_t; on varying these, one can achieve the best agreement with experiment. It should be clear, however, that these asymptotic expressions are correct only in the neighbourhood of small $\tau=(\Phi_\theta-\Phi)/\Phi$ and large N, whereas the numerical experiment yields data mainly in the region of small N and large τ. Therefore, the best coincidence with numerical data does not always ensure correct determination of Φ_θ, ν_t, φ_t (see ref. 54). An important part here may be played by the unknown corrections to scaling, which can hardly be taken into account. We suppose, however, that it is not expedient to begin with the question about the corrections to scaling before the values of Φ_θ and ν_t have been determined. Moreover, the present work shows that our method of determination of the main tricritical exponent ν_t is practically independent of the corrections to scaling, which have different magnitudes for different lattices.

On the contrary, we suppose that it is not correct to use the values of ν_t and φ_t that have already been obtained by some other methods (say, by the ε-expansion method) and then, for better agreement with numerical data, introduce the corrections to scaling, as has been done in ref. 31. These corrections may completely suppress all the information contained in the numerical data. The corrections to scaling are discussed in detail in Appendix 3.

Thus, we begin to analyse the numerical data using the following simple scaling equation[12] as a starting point:

$$\langle X^2 \rangle = N^{2\nu_t} f_X(N^{\varphi_t}\tau) \quad (20)$$

where $\langle X^2 \rangle$ is the mean dimension of a chain ($\langle R^2 \rangle$ or $\langle S^2 \rangle$ depending on context) and τ is reduced temperature, $\tau=(\Phi_\theta-\Phi)/\Phi$. We assume the function $f_X(y)$ to be positive, twice continuously differentiable and monotonic, $df_X(y)/dy>0$. Hence, $2\tilde{\nu}_X(N)$, the tangent of the slope of the dependence of $\ln\langle X^2 \rangle$ on $\ln N$, is determined by the equation:

$$2\tilde{\nu}_X(y)=\frac{d(\ln\langle X^2\rangle)}{d\ln N}=2\nu_t+2\varphi_t\frac{f_X'(y)}{f_X(y)}y$$
$$=2\nu_t+2\varphi_t\tilde{\mu}_X(y) \quad (21)$$

where $y=N^{\varphi_t}\tau$ and $\tilde{\mu}_X(y)=yf_X'(y)/f_X(y)$.

According to equations (1) and (2) the function $\tilde{\mu}_X(y)$ must have limits:

$$\lim_{y\to\infty}\tilde{\mu}_X(y)=\mu_+=(\nu-\nu_t)/\varphi_t\geqslant 0 \quad (22)$$

$$\lim_{y\to-\infty}\tilde{\mu}_X(y)=\mu_-=(1/d-\nu_t)/\varphi_t\leqslant 0 \quad (23)$$

By differentiating the function $2\tilde{\nu}_X(y(N))$ with respect to N, it can be shown that, when y is a sufficiently small positive number, the function $2\tilde{\nu}_X(y(N))$ is an increasing function of N, when y is small and negative, $2\tilde{\nu}_X(y(N))$ is a decreasing function of N, and when y is exactly equal to zero, $2\tilde{\nu}_X(y(N))$ is independent of N and equal to $2\nu_t$. It should be mentioned that the function $\tilde{\mu}_X(y)$, being monotonic within the neighbourhood of its single root $y=0$, may not be monotonic within its whole domain.

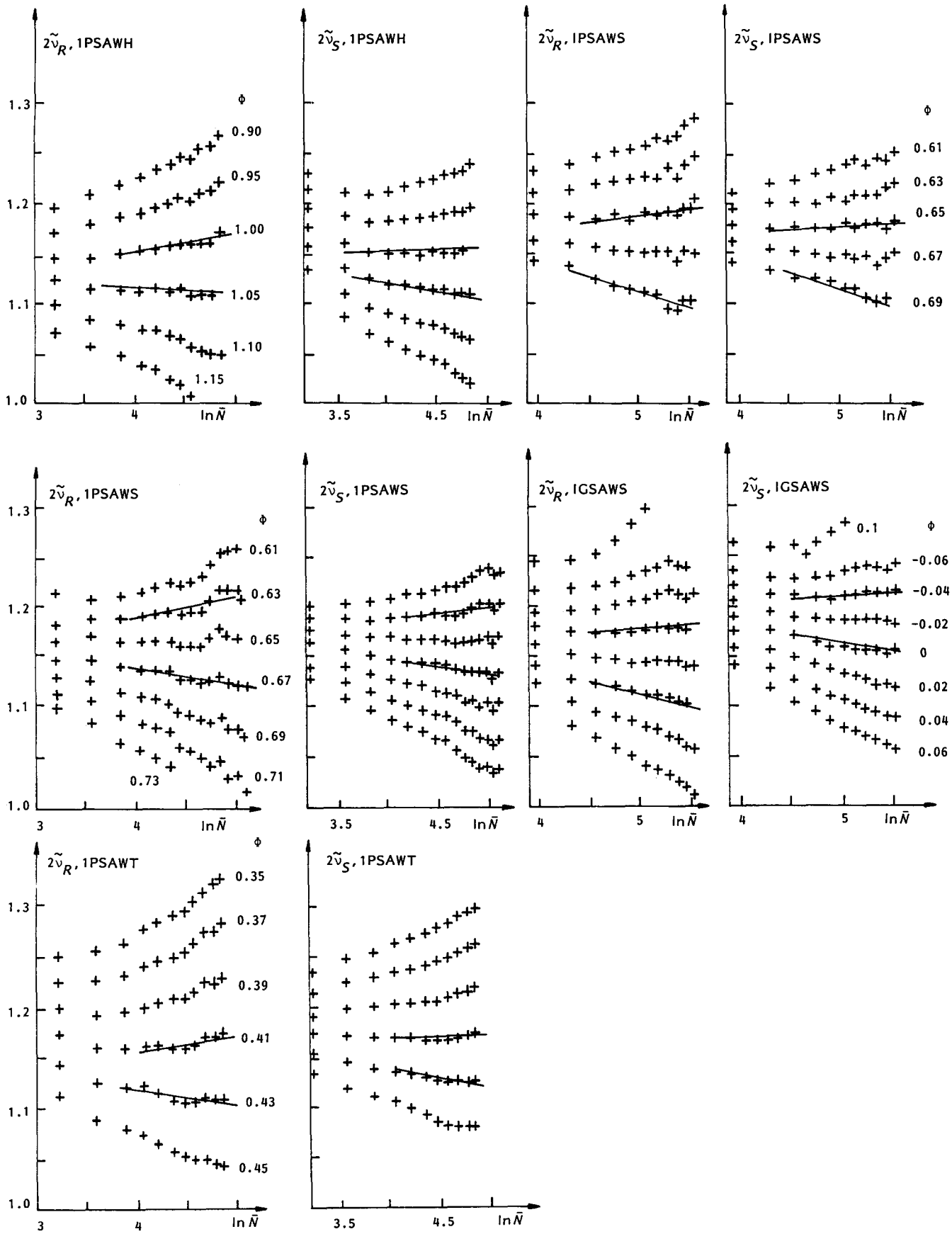

Figure 2 The dependences of the slopes $2\tilde{\nu}_R$ and $2\tilde{\nu}_S$ of parts of the curves $\ln\langle R^2\rangle(\ln N)$ and $\ln\langle S^2\rangle(\ln N)$ on the mean logarithm $\ln N$ of the chain lengths N for a given part of the curve at different values of Φ, which are shown on one of the plots for each model. The values of Φ vary with a small step in the neighbourhood of the θ point for each model. For a description of the straight lines, see the heading of *Table 2*. Parallel vertical axes have the same scales

Table 2 Results of graphical determination of the θ point and the exponent ν_t, using the dependences of the chain sizes $\langle R^2\rangle$ or $\langle S^2\rangle$ (*Figure 2*) or of their ratio (*Figure 3*) on the number of links N and the interaction parameter Φ for different models. (The data for the IGSAWS model are given in order to illustrate possible errors of the present method, because it is exactly known[5] for this model that $\Phi=0$ and $2\nu_t=8/7=1.143$)

Type of dependence	Quantity	1PSAWH	1PSAWT	1PSAWS	IPSAWS	IGSAWS
$\langle S^2\rangle$	Φ_θ^+	1.00	0.41	0.63	0.65	−0.04
	Φ_θ^-	1.05	0.43	0.67	0.69	0.00
	Φ_θ^0	1.015	0.415	0.654	0.658	−0.024
	Φ'_θ	1.023	0.425	0.667	0.672	0.010
	$2\tilde{\nu}_+$	1.152	1.171	1.192	1.178	1.210
	$\Delta\tilde{\nu}_+$	+0.006	+0.006	+0.020	+0.008	+0.008
	$2\tilde{\nu}_-$	1.114	1.130	1.140	1.114	1.156
	$\Delta\nu_-$	−0.014	−0.016	−0.014	−0.016	−0.012
	$2\tilde{\nu}_0$	1.141	1.160	1.161	1.165	1.188
$\langle R^2\rangle$	Φ_θ^+	1.00	0.41	0.63	0.65	−0.02
	Φ_θ^-	1.05	0.43	0.67	0.69	0.02
	Φ_θ^0	1.036	0.425	0.657	0.664	−0.009
	Φ'_θ	1.018	0.418	0.662	0.673	0.000
	$2\tilde{\nu}_+$	1.161	1.165	1.195	1.190	1.177
	$\Delta\tilde{\nu}_+$	+0.016	+0.014	+0.038	0.012	+0.008
	$2\tilde{\nu}_-$	1.113	1.110	1.131	1.109	1.110
	$\Delta\tilde{\nu}_-$	−0.006	−0.014	−0.018	−0.030	−0.022
	$2\tilde{\nu}_0$	1.126	1.138	1.152	1.167	1.156
$\langle R^2\rangle/$	$\Phi_\theta^\wedge$	1.05	0.42	0.65	0.68	−0.02
$6\langle S^2\rangle$	A_1	0.06±0.02	0.04±0.02	0.04±0.02	0.04±0.02	−0.01±0.04

Φ_-^+, Φ_-^- are the boundaries of Φ interval in which there is practically no dependence of $\tilde{\nu}$ on $\bar{N}$ at largest $\bar{N}$ (straight lines on *Figure 2*)
$\tilde{\nu}_+$, $\tilde{\nu}_-$ are $\tilde{\nu}$ values on the boundaries $\Phi_\theta^\pm$
$\Delta\tilde{\nu}_+$, $\Delta\tilde{\nu}_-$ are the corrections to $\tilde{\nu}_+$, $\tilde{\nu}_-$ values connected with the possible dependence of $\tilde{\nu}$ on $\bar{N}$
Φ_-^0, $2\tilde{\nu}_0$ are results of linear interpolation using the values $\Phi_\theta^\pm$, $\tilde{\nu}_\pm$, $\Delta\tilde{\nu}_\pm$
Φ'_- are the values of Φ at which $2\tilde{\nu}(N)\simeq 8/7$ (at large $\bar{N}$)

It can be derived from our numerical data that, at large negative values of y, $\tilde{\mu}_X(y)<\mu_-$ and, therefore, the function $\tilde{\mu}_X(y)$ must be decreasing in this region in order to satisfy condition (23). Passing through its minimum at some $y<0$, the function $\tilde{\mu}_X(y)$ tends from below to its limiting value μ_-. The effect of non-monotonic behaviour of the function $\tilde{\mu}_X(y)$, however, may arise due to corrections to scaling.

Thus, it follows from the above-mentioned assumptions that the dependence of the slope $2\tilde{\nu}_X(N)$ of the function $\ln\langle X^2\rangle(\ln N)$ must in the vicinity of the θ point change its character: $2\tilde{\nu}_X(N)$ must increase above ($T>\theta$ or $\Phi<\Phi_\theta$) and decrease with growing N below the θ point ($T<\theta$ or $\Phi>\Phi_\theta$). Exactly at the θ point $2\tilde{\nu}_X(N)$ must be equal to $2\nu_t$. These conditions give the opportunity for simultaneous determination of the θ point and the tricritical exponent ν_t.

The value of the slope $2\tilde{\nu}_X(N)$ was determined by means of the least-squares method, constructing a straight line by a group of $k=5$ or $k=3$ neighbouring points $\{\ln\langle X^2\rangle_i, \ln N_i\}_{i=1}^k$, minimizing the difference:

$$\delta^2=\sum_{i=1}^{k}\{\ln\langle X^2\rangle_i-2\tilde{\nu}_X(\bar{N})\ln N_i-B_X(\bar{N})\}^2 \quad (24)$$

where the value $\bar{N}$ is calculated by the equation:

$$\bar{N}=(N_1N_2\ldots N_k)^{1/k} \quad (25)$$

When an attempt was made to draw the straight line through each pair of neighbouring points, the statistical spread of the values of $2\tilde{\nu}_X(\bar{N})$ was too large. The plots of the obtained dependences $2\tilde{\nu}_X(\bar{N})$ at various values of Φ for different models are shown on *Figure 2* (see also analogous plots in ref. 3).

As can be seen from *Figure 2*, the behaviour of the dependence $2\tilde{\nu}_X(\bar{N})$ is really changing at some value of $\Phi=\Phi_\theta$, which is in complete agreement with the above-stated conjectures. The values of Φ_θ for different models differ from each other greatly but the values of $2\nu_t$ appear to be close to each other and lie in the interval between 1.13 and 1.18 (see *Table 2*). *Table 2* also contains the precise values of Φ_θ and $2\nu_t$ obtained by means of graphical linear interpolation, which using the slopes of the dependences of *Figure 2* finds the point Φ_θ^0 at which such a slope is approximately equal to zero when N is large. It is clear that one should take a rather cautious attitude to such interpolation, because for the IGSAWS model it gives negative Φ_θ^0, whereas it follows from general considerations[5] that for IGSAW Φ_θ must be exactly equal to zero, at this value of Φ the constant value of the free-energy exponent $\gamma_t=1$ is observed. Nevertheless, all the results obtained for all five models and for dependences of $\langle R^2\rangle$ as well as for dependences of $\langle S^2\rangle$ testify to the good agreement between obtained values of ν_t and, thus, confirm the hypothesis of the universality of the value $\nu_t=4/7$. The slight differences between these values may be due to the influence of the corrections to scaling at small N, which have different amplitudes for different lattices.

It should be mentioned that in the vicinity of the θ point the dependences $2\tilde{\nu}_X(\bar{N})$ for some models clearly

have non-monotonic behaviour. As a result, the precision of determination of Φ_θ and ν_t is not high. This non-monotonicity can be decreased by processing the data using the value $N+\kappa$ instead of N, where κ is a value of the order of unity, which is different for different models. Such a procedure is equivalent to the introduction of an analytical correction to scaling and cannot serve as a guarantee of the precision of the results as well. It seems more reasonable to advance towards the region of large N, ignoring at the same time the data for short chains. For example, it is difficult for the IPSAWS model to choose between the values 0.65 or 0.67 for the value Φ_θ. When $\Phi=0.65$, the values of $2\tilde{\nu}_R(\bar{N})$ have within the whole interval $51<\bar{N}<260$ less changes than when $\Phi=0.67$, but begin to grow at large N; whereas when $\Phi=0.67$, the values of $2\tilde{\nu}_R(\bar{N})$ decrease considerably at small $\bar{N}$ but become almost constant and equal to 1.15 when $\bar{N}>100$, which is in good agreement with the theoretical value of $2\nu_t=8/7\approx1.143$.

An analogous but even more expressive picture can be observed in the case of the IGSAWS model. The dependence $2\tilde{\nu}_R(N)$, obtained in our numerical experiment, undergoes the least changes at $\Phi=-0.02$, whereas at the apparent θ point at $\Phi=0.0$ it is decreasing until $\bar{N}=150$, and only when $\bar{N}>150$ is it practically constant and very close to the hypothetical value $2\nu_t=8/7$.

One more quantity through the changes of which one can judge about the location of the θ point is the universal ratio $B=\langle R^2\rangle/6\langle S^2\rangle$; see ref. 17. *Figure 3* illustrates the dependence of the quantity $A=\ln B$ on the length of the chain N. According to the predictions of ref. 17, this quantity must be well behaved at large N and small τ as:

$$A=-A_1+A_2N^{\varphi_t}\tau \tag{26}$$

where A_1, A_2 are small positive numbers. According to this equation, A must increase with increase of N above and decrease below the θ point. The curves on *Figure 3* must be concave above and convex below the θ point. Indeed, it is these very effects that can be observed on *Figure 3* for all models. Moreover, the value of parameter $\Phi=\Phi_\theta^A$ at which the quantity A is practically constant at large N is very close to Φ_θ, obtained by the previous method (see *Table 2*). The values of the constant A_1 are spread between 0.06 ± 0.02 for the 1PSAWH model and -0.01 ± 0.04 for the IGSAWS model, which contradicts the predictions of the ε-expansion method, according to which $A_1\approx0.2$. It is possible that the constant A_1 is universal for all these models, because the observed values of A for different models may tend to the same limit when N tends to infinity, but from different sides and at different speeds.

Unfortunately, our data on the mean number of contacts and specific heat (for the IPSAWS model they are discussed in ref. 3) do not allow us to determine with sufficient accuracy the location of the θ point. We can assert only that these data do not contradict the values of Φ_θ, obtained by previous methods. As a whole, our results for different models do not contradict (as can be seen from *Table 2*) the hypothesis of the universality of the value $2\nu_t=8/7$, rejecting undoubtedly values less than 1.1 or greater than 1.2.

INVESTIGATION OF THE FREE ENERGY

Another important characteristic of the coil–globule transition is the free energy, whose asymptotic behaviour also undergoes great changes in the vicinity of the θ point.

Let the absolute value of the free energy be defined as:

$$F=\ln\langle Z\rangle \tag{27}$$

where $\langle Z\rangle$ is an estimate of the partition function, obtained by equation (10). According to general scaling concepts (see for example refs. 55 and 56), the partition function $Z(N,\Phi)$ of an ensemble of chains of the length N with one fixed end can be written in the form:

$$Z(N,\Phi)=N^{\gamma_t-1}f_Z(N^{\varphi_t}\tau)\,e^{N\omega(\Phi)} \tag{28}$$

where γ_t is the tricritical exponent of the free energy, whose value is to be determined by means of the numerical experiment, τ is the reduced temperature, $\tau\sim(\Phi_\theta-\Phi)$, φ_t is the crossover exponent (see equation (20)), $\omega(\Phi)$ is an infinitely differentiable function, which is of no importance in the neighbourhood of the θ point but is necessary in the region of large $|\Phi|$ in order to obtain reasonable limits of $Z(N,\Phi)$ when $\Phi\to\pm\infty$, and $f_Z(y)$ is an infinitely differentiable function of scaling variable $y=N^{\varphi_t}\tau$, which has the following asymptotes for $y\to\pm\infty$:

$$f_Z(y)\sim\begin{cases}\exp(C_1y^{1/\varphi_t})y^{(\gamma-\gamma_t)/\varphi_t} & y\to+\infty\\ \exp(C_2y^{1/\varphi_t}+C_3y^{\rho/\varphi_t}) & y\to-\infty\end{cases} \tag{29}$$

where C_1, C_2, C_3 are constants, γ is the critical exponent of the free energy for the region of good solvents, whose exact value is equal to 43/32 (ref. 14), and ρ is an exponent that determines the power growth of the surface free energy of globules:

$$F_s(N^{\varphi_t}\tau)=C_3N^{\rho}\tau^{\rho/\varphi_t}\quad C_3<0,\ 0<\rho<1 \tag{30}$$

Taking logarithms of both sides of (28), we obtain that the free energy at large N has, in solvents of different quality, namely good ($\Phi<\Phi_\theta$), theta ($\Phi=\Phi_\theta$) and poor ($\Phi>\Phi_\theta$), the following asymptotes:

$$F(N,\Phi)=\text{const}+F_0(\Phi)N+\begin{cases}(\gamma-1)\ln N+o(1) & \Phi<\Phi_\theta\\ (\gamma_t-1)\ln N+o(1) & \Phi=\Phi_\theta\\ (C_3\tau^{\rho/\varphi_t}N^{\rho}+o(N^{\rho}) & \Phi>\Phi_\theta\end{cases} \tag{31}$$

where $F_0(\Phi)$ is the reduced free energy per link in the limit of $N\to\infty$, being equal to the logarithm of the *effective coordination number* $\tilde{z}(\Phi)$.

According to equation (29), the quantity $d^2F_0/d\Phi^2$ must in the neighbourhood of the θ point obey the power law:

$$\frac{d^2F_0(\Phi)}{d\Phi^2}\sim\begin{cases}C_1K_t(K_t-1)|\Phi-\Phi_\theta|^{K_t-2} & \Phi<\Phi_\theta\\ C_2K_t(K_t-1)|\Phi-\Phi_\theta|^{K_t-2} & \Phi>\Phi_\theta\end{cases} \tag{32}$$

where $K_t=1/\varphi_t$ is the order of the phase transition in the limit $N\to\infty$. In the case of very large values of Φ, when the main contribution to the free energy is due to the most dense conformations, the quantity $F_0(\Phi)$ must behave as:

$$F_0(\Phi)=\Phi(z-2)/2+S_0+\omega_1(\Phi) \tag{33}$$

where $\Phi(z-2)/2$ is the internal energy of the monomer, being inside the globule, S_0 is an entropy term, proportional to the logarithm of the number of most dense conformations per link, and the function $\omega_1(\Phi)$ tends to zero when $\Phi\to\infty$.

It is more convenient for numerical investigation of

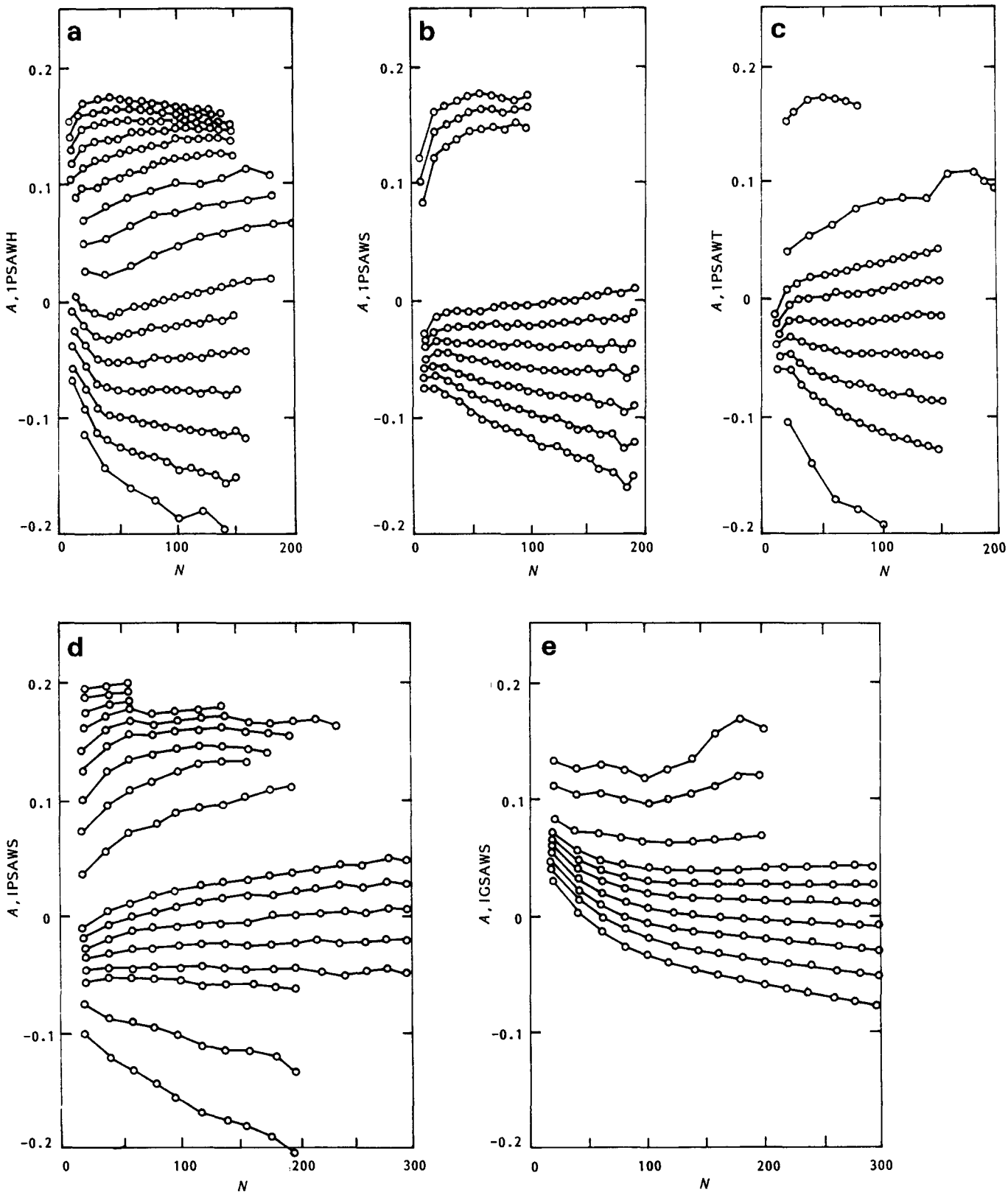

Figure 3 The dependences of A (the logarithm of the universal ratio, $A=\ln[\langle R^2\rangle/6\langle S^2\rangle]$) on the chain length N for different models and at different values of the interaction parameter Φ, which are the following: (a) for the model 1PSAWH, $\Phi=0$, 0.1, 0.2, 0.3, 0.4, 0.5, 0.6, 0.7, 0.8, 0.9, 0.95, 1.0, 1.05, 1.1, 1.15, 1.120; (b) for the model 1PSAWS, $\Phi=0.0$, 0.1, 0.2, 0.61, 0.63, 0.65, 0.67, 0.69, 0.71, 0.73; (c) for the model 1PSAWT, $\Phi=0.0$, 0.3, 0.35, 0.37, 0.39, 0.41, 0.43, 0.45, 0.5; (d) for the model IPSAWS, $\Phi=-0.3$, -0.2, -0.1, 0.0, 0.1, 0.2, 0.3, 0.4, 0.5, 0.61, 0.63, 0.65, 0.67, 0.69, 0.7, 0.75, 0.8; (e) for the model IGSAWS, $\Phi=-0.3$, -0.2, -0.1, -0.06, -0.04, -0.02, 0.00, 0.02, 0.04, 0.06. For all the models the values of A decrease with the growth of Φ

the free energy to consider the derivative of the free energy with respect to the chain length N, dF/dN, which can be defined in the numerical experiment as the finite difference:

$$\Delta F_{2k}=\frac{1}{2k}[F(N+k,\Phi)-F(N-k,\Phi)] \qquad (34)$$

As follows from equations (28) and (29), the slope of the dependence of ΔF_{2k} *versus* $\lambda=1/N$, constructed at different values of Φ, depends only on the scaling variable $y=N^{\varphi_t}\tau$. Therefore, the quantity ΔF_{2k} can be expressed in the form:

$$\Delta F_{2k}(\lambda,\Phi)=F_0+\int_0^{\lambda}\tilde{\gamma}(\tau/\lambda'^{\varphi_t})d\lambda' \qquad (35)$$

where $\tilde{\gamma}(\tau/\lambda'^{\varphi_t})$ is the above-mentioned slope, which, according to the equations (28) and (29), obeys the following relations:

$$\tilde{\gamma}(0)=\gamma_t-1 \quad \lim_{y\to\infty}\tilde{\gamma}(y)=\gamma-1$$

$$\lim_{y\to-\infty}[\tilde{\gamma}(y)/|y|^{\rho/\varphi_t}]=C_3\rho(1-\rho)<0 \qquad (36)$$

In a good solvent, when $y\gg1$, the dependences $\Delta F_{2k}(\lambda)$ must be practically linear with slope $\gamma-1$. As we approach the θ point the dependences become convex and their slope decreases from $\gamma-1$ at small λ to γ_t-1 at large λ. Exactly at the θ point the dependence again becomes linear with slope γ_t-1. Below the θ point ($y<0$) the curves become concave and their slope $\tilde{\gamma}(\lambda)$ increases from $-\infty$ when $\lambda\to0$ to γ_t-1 at large λ. Thus, these dependences allow us to define simultaneously the location of the θ point and the value of the exponent γ_t, as was done above for the exponent ν_t by means of dependences $\ln\langle X^2\rangle(\ln N)$.

Figure 4 shows the dependences ΔF_{2k} *versus* λ within the whole interval of investigated values of Φ for the models 1PSAWS and IPSAWS. Note first of all that in *Figure 4* all the above-mentioned effects can be observed. At small Φ the curves on *Figure 4* are straight parallel lines with slope $\tilde{\gamma}$ that is close to $\gamma-1=11/32$. The intersection points of those lines with the y axis yield the values of $F_0(\Phi)$. At $\Phi=0$ the data for $\tilde{\gamma}$ and $F_0(0)$ practically coincide for both models and yield $\gamma=0.34\pm0.01$, $F_0(0)=0.97\pm0.0005$ or $\tilde{z}_S(0)=2.638\pm0.001$; cf. ref. 57. Analogous studies give for the triangular (1PSAWT model) and honeycomb lattices (1PSAWH model) $\tilde{\gamma}=0.34\pm0.02$, $\tilde{z}_T(0)=4.152\pm0.002$ and $\tilde{\gamma}=0.33\pm0.02$, $\tilde{z}_H(0)=1.847\pm0.001$ respectively. As Φ approaches Φ_θ the slope of the curves on *Figure 4* decreases with growth of λ from its maximum value, attained at small λ, which is very close to $\gamma-1=11/32$ at first, but rapidly diminishing as Φ becomes closer to Φ_θ. At $\Phi=0.67$, the curve is practically straight and horizontal. Above $\Phi=0.67$ the slope of the curves becomes negative and its absolute value tends to grow with decrease of λ. Unfortunately, this tendency is not very pronounced, because of the great statistical spread of the data at large values of Φ and N. For the same reason, we cannot separate strictly the regions of concave and convex curves and therefore we cannot determine the value Φ_θ by the analysis of the free energy as precisely as has been done by the analysis of sizes in an earlier section. That is why the confidence interval of determination of Φ_θ by means of the free energy is rather wide and includes the values of Φ_θ summarized in *Table 2* as well as the value Φ_{θ_1} for which the slope of the dependence of ΔF_{2k} *versus* λ is equal to zero. *Figure 5* shows the analogous dependences for all the models within a narrow interval of Φ including the θ point. In order to determine the exponent γ_t we calculate the slopes $\tilde{\gamma}_+$ and $\tilde{\gamma}_-$ of the curves at $\Phi=\Phi_\theta^+$ and $\Phi=\Phi_\theta^-$, respectively (see *Table 2*). In all cases $\tilde{\gamma}_-<0<\tilde{\gamma}_+$, and therefore the value Φ_{θ_1} belongs to the interval between Φ_θ^+ and Φ_θ^-, whereas the value $\gamma=8/7$, proposed in ref. 2, is always greater than $\tilde{\gamma}_+$. The results of the determination of the values Φ_{θ_1} and γ_+ for different models are summarized in *Table 3*. It can be seen from

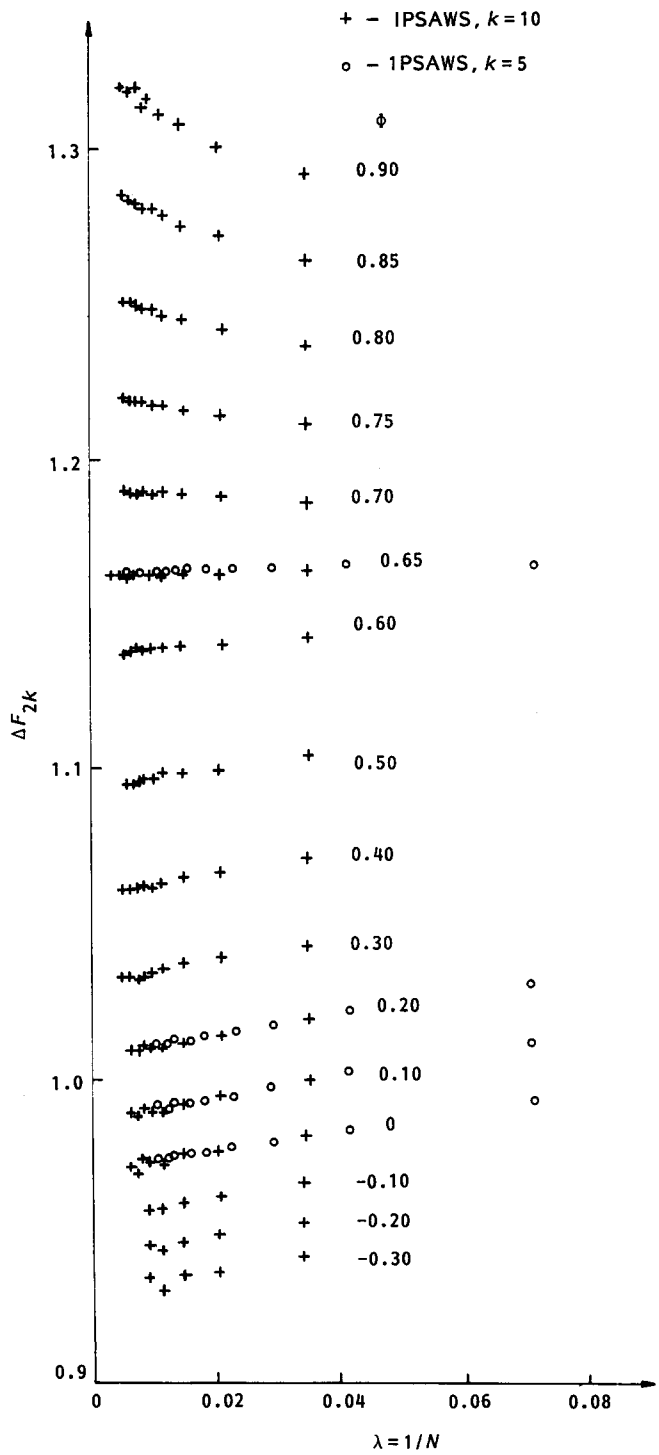

Figure 4 The dependences of ΔF_{2k} on $\lambda=1/N$ for the IPSAWS and 1PSAWS models at different values of Φ, shown on the plot

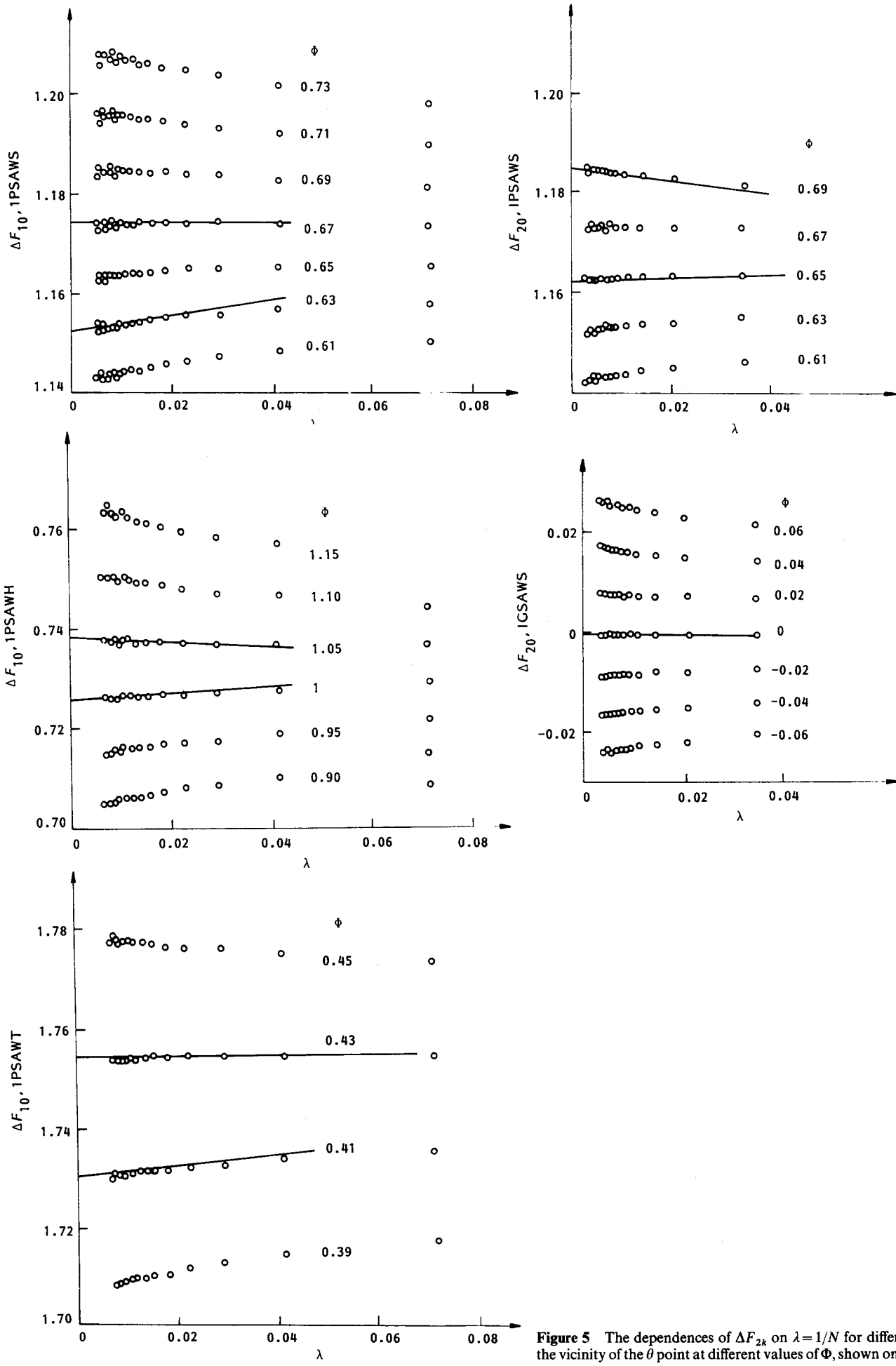

Figure 5 The dependences of ΔF_{2k} on $\lambda = 1/N$ for different models in the vicinity of the θ point at different values of Φ, shown on the plots

Table 3 Determination of the free-energy exponent for different models. The values of $\tilde{\gamma}_+$ and $\tilde{\gamma}_-$ are the upper and lower estimates of the exponent $\gamma_t - 1$ and correspond to the values of interaction parameter $\Phi = \Phi_\theta^+$ and $\Phi = \Phi_\theta^-$, determined in *Table 2*. The quantity Φ_{θ_1} is the value of Φ at which $\gamma_t = 1$. The quantity $\tilde{z}(\Phi_{\theta_1})$ is the value of effective coordination number $\tilde{z}$, which corresponds to $\Phi = \Phi_{\theta_1}$

Quantity	1PSAWH	1PSAWT	1PSAWS	IPSAWS
$\tilde{\gamma}_+$	0.04 ± 0.02	0.10 ± 0.02	0.12 ± 0.04	0.08 ± 0.02
$\tilde{\gamma}_-$	-0.05 ± 0.02	0.01 ± 0.02	0.00 ± 0.02	-0.12 ± 0.02
Φ_{θ_1}	1.03 ± 0.02	0.43 ± 0.01	0.67 ± 0.01	0.67 ± 0.01
$\tilde{z}(\Phi_{\theta_1})$	$2.08 + 0.01$	5.78 ± 0.01	3.23 ± 0.01	3.23 ± 0.01

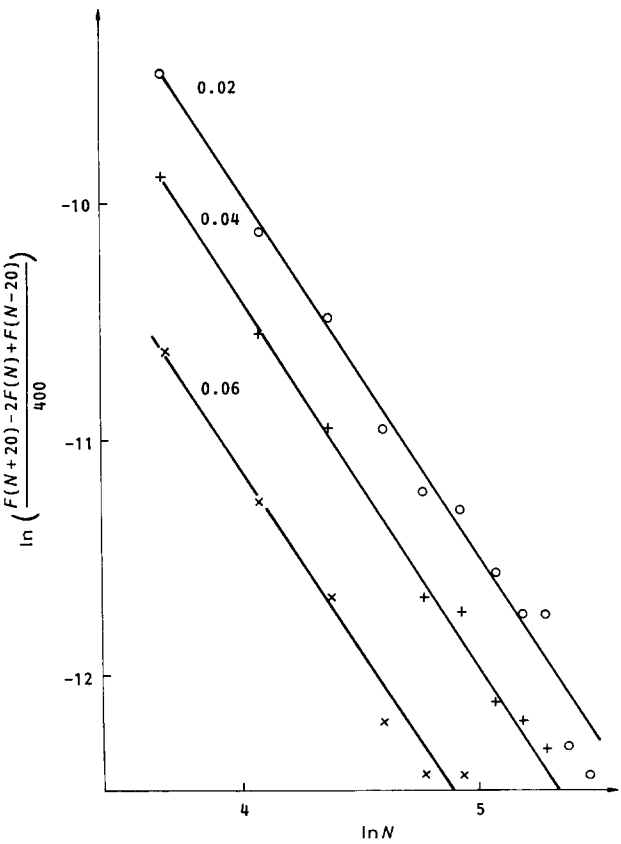

Figure 6 The dependences of the logarithm of the finite difference for the second derivative of the free energy d^2F/dN^2 on the chain length N for the IGSAWS model at positive values of parameter Φ, shown on the plot

Tables 2 and *3* that the values Φ_{θ_1} at which the slopes of the dependences $\Delta F_{2k}(\lambda)$ of *Figure 5* are close to zero at small λ practically coincide with the values Φ'_θ at which the slopes of the dependences of $\ln\langle X^2\rangle$ *versus* $\ln N$ at large N are close to 8/7. That is why the equation $\gamma_t = 1$, which is exact for the IGSAW model, may be correct for the other models as well. Finally, we can assert with a high degree of reliability that for all the models the values of γ_t lie within the interval between 0.98 and 1.08, which is in good agreement with the results of other work[6,7].

Let us dwell now upon the determination of the *effective coordination number* $z(\Phi)$ when $\Phi \ll \Phi_\theta$. The value $F_0(\Phi)$ can be determined with sufficient accuracy by means of linear extrapolation of the dependence $\Delta F_{2k}(\lambda)$ for $\lambda \to 0$. For larger Φ but still above the θ point, the slope of these dependences undergoes considerable changes at small λ and so linear extrapolation becomes impossible. We may try to perform quadratic extrapolation, postulating that at $\lambda = 0$ the slope of the curves is exactly equal to 11/32, when $\Phi < \Phi_\theta$, and that at small λ the function $\Delta F_{2k}(\lambda)$ can be written in the form

$$\Delta F_{2k} = F_0(\Phi) + \frac{11}{32}\lambda + b_2\lambda^2$$

The result of the quadratic extrapolation will be the arithmetic mean of the results of linear extrapolations with the theoretical slope 11/32 and with the greatest slope, attained in the numerical experiment at small λ. It is clear, however, that in the close vicinity of the θ point the quadratic extrapolation also ceases to yield the necessary accuracy. When $\Phi > \Phi_\theta$ we can perform reliable linear extrapolation plotting the data against $\lambda^{1-\rho}$ instead of λ. But in order to do that it is necessary to know the value of the exponent ρ, which can be determined from the slope of the dependence of $\ln[d^2F(N,\Phi)/dN^2]$ on $\ln N$. The dependences of the corresponding finite difference $\ln\{(1/k^2)[F(\Phi,N+k) - 2F(\Phi,N) + F(\Phi,N-k)]\}$ on $\ln N$ for the IGSAWS model at different $\Phi > 0$ are shown on *Figure 6*. The slopes of these lines must be equal to $\rho - 2$, from which it follows that $\rho = 0.53 \pm 0.05$. It is impossible to determine ρ in this way for other models because of a very large statistical spread of the data at large N and Φ.

The dependences of $|\Delta F_{2k}|$ on $\lambda^{1/2}$ for the IGSAWS model are plotted on *Figure 7*. It can be seen that at

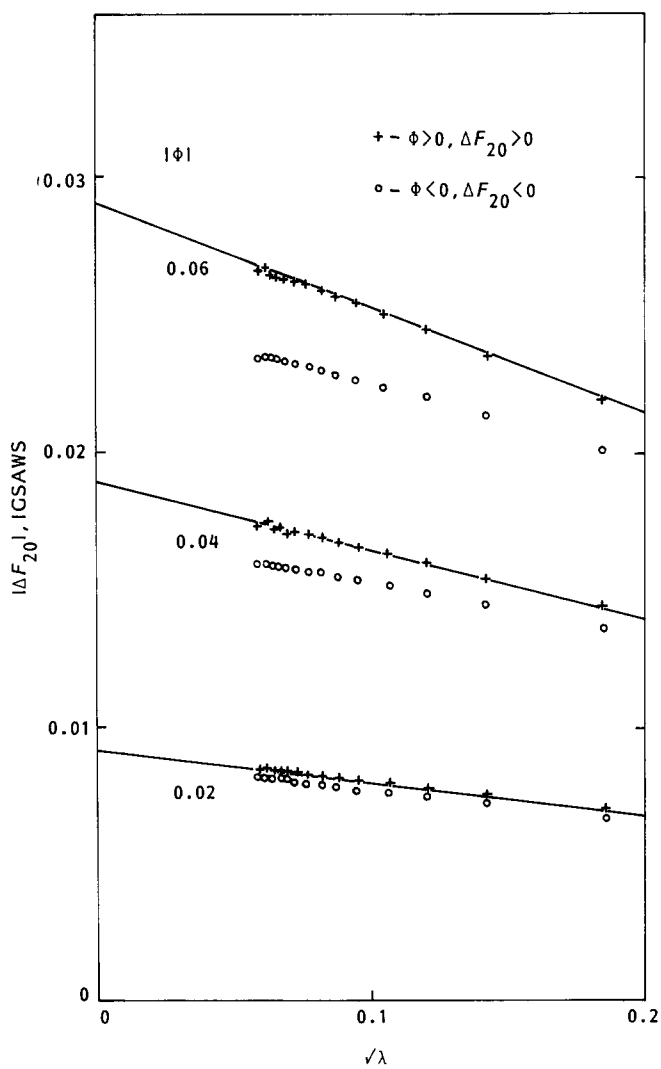

Figure 7 The dependences ΔF_{2k} on $\lambda^{1/2}$ for the IGSAWS model at different values of Φ, shown on the plot

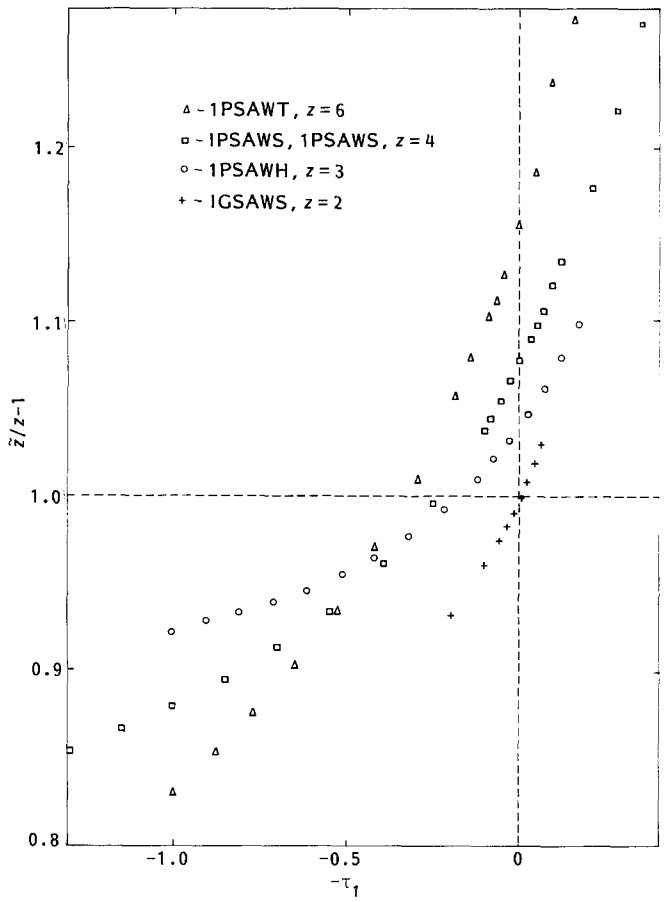

Figure 8 The dependences of the reduced coordination number $\tilde{z}/(z-1)$ on the reduced temperature τ_1. For the IGSAWS model $\tau_1=-\Phi$, for the other models $\tau_1=(\Phi_{\theta_1}-\Phi)/\Phi_{\theta_1}$. For the IGSAWS model the coordination number z is formally equated to 2, so that $1/(z-1)=1$

$\Phi>0$ they are practically linear, whereas at $\Phi<0$ their slopes decrease when $\lambda\to 0$, which is in complete agreement with theoretical predictions. Moreover, when $\Phi>0$, the slope of the dependences of ΔF_{2k} on $\lambda^{1/2}$ depends almost proportionally on Φ. More accurate logarithmic constructions yield that the slope $d(\Delta F_{2k})/d(\lambda^{1/2})$ depends on τ as $\tau^{1.05\pm 0.05}$, and, hence, according to equation (31), one can conclude that $\rho/\varphi_t=1.05$ or $\varphi_t=0.5\pm 0.08$. From *Figure 7* one can also determine the values of $F_0(\Phi)$ at $\Phi>\Phi_\theta$. When $\Phi<\Phi_\theta$, the values of $F_0(\Phi)$ can be determined from *Figure 5* by means of quadratic extrapolation. Finally, we have for the IGSAW model a set of sufficiently accurate values of the function $F_0(\Phi)$ within the neighbourhood of the θ point: $F_0(-0.06)=-0.0246$, $F_0(-0.04)=-0.0170$, $F_0(-0.02)=-0.0088$, $F_0(0.00)=0.0000$, $F_0(0.02)=0.0092$, $F_0(0.04)=0.0189$, $F_0(0.06)=0.0291$.

Plotting the dependence of $\ln[F_0(\Phi+\Delta\Phi)+F_0(\Phi-\Delta\Phi)-2F_0(\Phi)]$ on $\ln|\Phi|$, we obtain, according to equation (32), that the order K_t of the phase transition for the IGSAW model is not less than 2 ($K_t\geqslant 2$), from which it follows that $\varphi_t\leqslant 0.5$. Unfortunately, it is impossible to perform such constructions for other models, because we know exactly neither the values of $F_0(\Phi)$ nor the values of Φ_θ. It should be mentioned that the value $\rho=0.5$, obtained for the IGSAWS model, is in excellent agreement with the mean-field prediction according to which the surface of the globule grows as the square root of the number of its monomers. Assuming that this mean-field value $\rho=1/2$ is correct not only in the case of IGSAWS, we construct plots analogous to that of *Figure 7* and find with their help the functions $\tilde{z}(\Phi)$ at $\Phi>\Phi_0$ for all the other models. *Figure 8* illustrates the dependences of the quantity $\tilde{z}(\Phi)/(z-1)$ on τ_1, where z is the coordination number of the lattice and $\tau_1=(\Phi_{\theta_1}-\Phi)/\Phi_\theta$ for all the models except IGSAWS and $z=2$, $\tau_1=-\Phi$ for the IGSAW model. The values of Φ_{θ_1} are taken from *Table 3*. It is the proximity of the values of $\tilde{z}(\Phi)$ for the IPSAWS and 1PSAWS models that attracts attention in *Figure 8*. This proximity confirms the hypothesis, based on self-similarity, which predicts the equivalence of these two models in the limit $N\to\infty$.

The dependences of the slope $\tilde{\gamma}$ on the scaling variable $y=\tau_1 N^{1/2}$, constructed with the help of plots of the quantity ΔF_{2k} *versus* λ (see *Figures 4* and *5*), are shown on *Figure 9a* for the IGSAW model and on *Figure 9b* for all other models. (It is assumed that $\varphi_t=0.5$ in all cases.) These dependences of *Figure 9* show the universality of the function $\gamma(y)$ for different types of lattices as well as good agreement with theoretical predictions (see equations (35) and (36)). It is to be mentioned that all dependences of *Figure 9* were plotted in such a way that each of them passes through the origin. That is why this figure cannot be used as a proof of the exact equality $\gamma_t=1$, but still we can affirm that the exact value of γ_t is very close to unity, and in any case is considerably less than 8/7, which is the value of the exponent γ_t for the model of Duplantier and Saleur (DS). There is an even larger discrepancy between the DS model and the 1PSAWS model, constructed at $\Phi\approx\Phi_\theta\approx 0.65$ with each chain starting from the origin and confined on the half-plane $x\geqslant 0$ (see refs. 52 and 53). The dependence of ΔF_{2k} on λ for this model is shown in *Figure 10*. Its slope yields the value of the exponent γ_{1t} close to 0.5, whereas according to ref. 2 $\gamma_{1t}=8/7$. These discrepancies may be explained by the less universality of the exponent of the free energy than that of the fractal dimensionality $1/\nu_t$. In connection with this problem we ought to mention some very interesting works[8–11,27,58] on renormalization group theory in which the possibility of the existence of other universality classes, corresponding to the θ point in two dimensions, is discussed.

DETERMINATION OF THE CROSSOVER EXPONENT φ_t AND CONSTRUCTION OF THE SCALING FUNCTIONS

The analysis of the free energy in the previous section has shown that the value of the crossover exponent φ_t is close to 0.5. Let us dwell upon the more detailed determination of the exponent φ_t, based on the analysis of conformational characteristics whose dependence on N and Φ is described, if one neglects corrections to scaling, by equation (20). Actually, it follows from equation (20) that:

$$(\partial \ln\langle X^2\rangle/\partial\Phi)|_{\Phi=\Phi_\theta}=\text{const}\times N^{\varphi_t} \tag{37}$$

$$(\partial\langle X^2\rangle/\partial\Phi)|_{\Phi=\Phi_\theta}=\text{const}\times N^{2\nu_t+\varphi_t} \tag{38}$$

That is why, constructing plots of the dependences of the quantities:

$$Y_X(\Phi_1,\Phi_2,N)=\ln\left(\frac{1}{|\Phi_1-\Phi_2|}\,|\ln\langle X^2(\Phi_1,N)\rangle-\ln\langle X^2(\Phi_2,N)\rangle|\right) \tag{39}$$

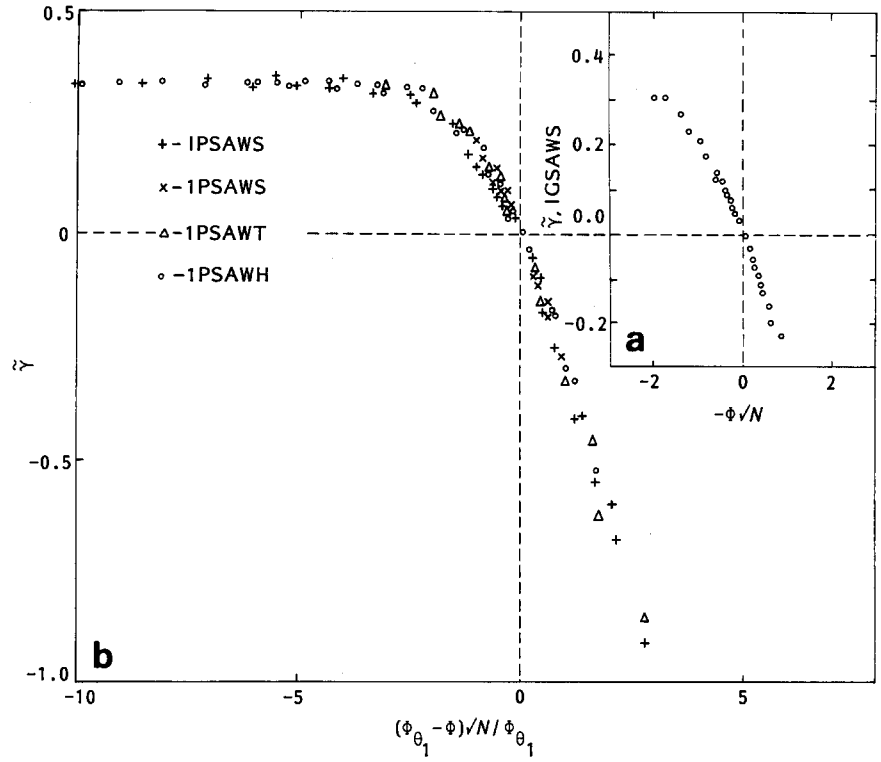

Figure 9 The scaling functions $\tilde{\gamma}(y)$ vs. scaling variable $y=N^{1/2}\tau_1$ for the IGSAWS model (a) and for all the other models (b)

and

$$\tilde{Y}_X(\Phi_1,\Phi_2,N) = \ln\left(\frac{1}{|\Phi_1-\Phi_2|}|\langle X^2(\Phi_1,N)\rangle-\langle X^2(\Phi_2,N)\rangle|\right) \quad (40)$$

on $\ln N$ with Φ_1 and Φ_2 close to Φ_θ, we can determine from their slopes the approximate values of φ_t and $2\nu_t+\varphi_t$, respectively. The dependences of $Y_X(\Phi_1,\Phi_2,N)$ *versus* $\ln N$ for different models are shown on *Figure 11a*. It appears that the values of the slope $\partial Y_X(\Phi_1,\Phi_2,N)/\partial \ln N$ are almost independent of Φ_1 and Φ_2 in the vicinity of the θ point, and the slope itself is decreasing slightly with growth of $\ln N$. Its value at large $\ln N$ yields an estimate of the value φ_t. This value for different models varies from 0.57 (1PSAWS, $\langle X^2\rangle=\langle S^2\rangle$) to 0.45 (IPSAWS, $\langle X^2\rangle=\langle R^2\rangle$) (see *Table 4*). We have also obtained similar values of φ_t (see *Table 4*), constructing the plots of dependences $\tilde{Y}_X(\ln N)$ (see *Figure 11b*) and subtracting the value of the slope $\partial\tilde{Y}_X/\partial \ln N$ of the dependence of $\tilde{Y}_X(\Phi_1,\Phi_2,N)$*versus* $\ln N$ from the value of the slope $2\tilde{\nu}_X=\partial\ln\langle X^2\rangle/\partial\ln N$ of the dependence $\ln\langle X^2\rangle(\ln N)$ at $\Phi=(\Phi_1+\Phi_2)/2$, both slopes being determined at the largest values of $\ln N$ attained in our numerical experiment. Naturally, this method is less accurate than the first one, because it involves subtraction of two values that are close to each other, both being determined with some error. It is interesting to note (see *Figure 11b*) that the values Y_X for all the models of walks on the square lattice (1PSAWS, IPSAWS and IGSAWS) are very close to each other.

The third method of determination of φ_t has been developed from the graphical method proposed in our previous papers[3,4,33]. *Figure 12* shows a typical example of the dependences of $(\ln\langle X^2\rangle-2\tilde{\nu}_t\ln N)$ on $\ln N$, obtained at several values of Φ, close to Φ_θ, and the value

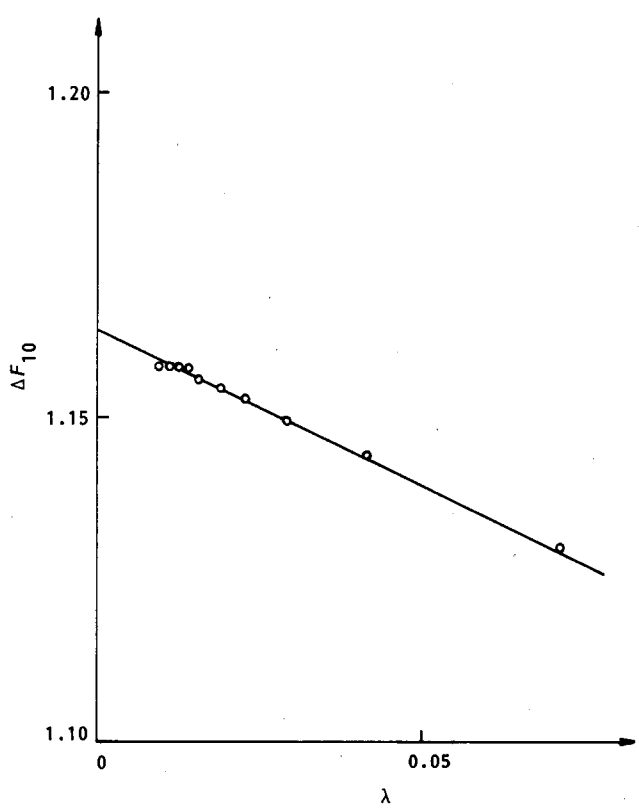

Figure 10 The dependence of ΔF_{10} on reciprocal chain length $\lambda=1/N$ for the 1PSAWS model on the half-plane. The slope of the straight line is approximately equal to the exponent $\gamma_{11}-1=-0.5$

of $2\tilde{\nu}_t$ being chosen from the interval between the values $2\tilde{\nu}_+$ and $2\tilde{\nu}_-$, shown in *Table 2*.

Those curves on *Figure 12* that belong to the region above the θ point ($\Phi<\Phi_\theta$) appear to be increasing and

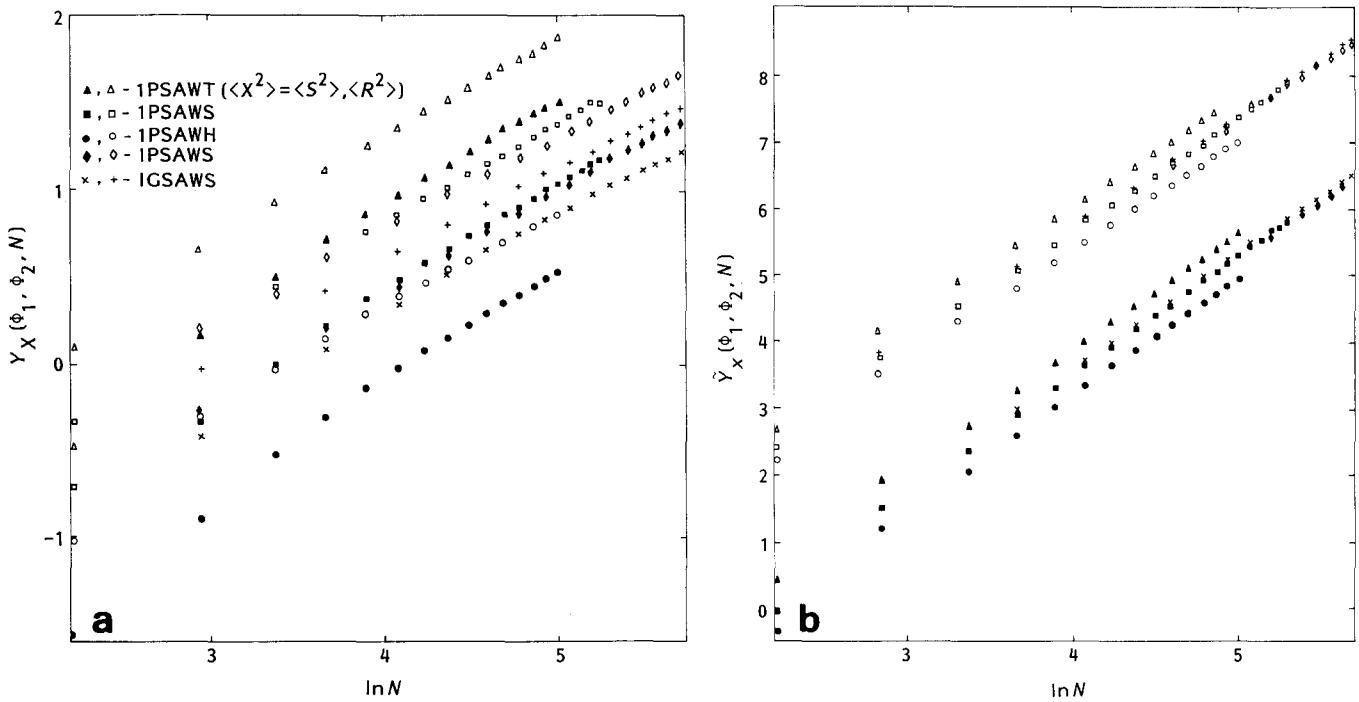

Figure 11 The dependences of (a) the logarithmic and (b) the ordinary derivative of the chain sizes $\langle R^2 \rangle$ and $\langle S^2 \rangle$ with respect to the interaction parameter Φ, on the length of the chain N, constructed in the double-logarithmic scale for different models. The derivatives are calculated by means of the method of finite differences (see equations (39) and (40)) for two values of $\Phi = \Phi_1$ and $\Phi = \Phi_2$ in the vicinity of the θ point: for the 1PSAWS and IPSAWS models $\Phi_1 = 0.65$, $\Phi_2 = 0.67$, for the IPSAWH model $\Phi_1 = 1.0$, $\Phi_2 = 1.05$, for the IGSAWS model $\Phi_1 = -0.02$, $\Phi_2 = 0.0$ and for the 1PSAWT model $\Phi_1 = 0.41$, $\Phi_2 = 0.43$

Table 4 Determination of the crossover exponent φ_t for different models, using different methods and different dependences $\langle S^2 \rangle$ or $\langle R^2 \rangle$ on N and Φ: the first method (I) by equation (39), the second method (II) by equation (40) and the third method (III) by equation (41)

Number of method	Type of dependence	1PSAWH	1PSAWT	1PSAWS	IPSAWS	IGSAWS
I	$\langle S^2 \rangle$	0.56	0.51	0.55	0.49	0.49
		±0.03	±0.03	±0.03	±0.03	±0.03
	$\langle R^2 \rangle$	0.49	0.53	0.57	0.45	0.48
		±0.03	±0.03	±0.03	±0.03	±0.03
II	$\langle S^2 \rangle$	0.58	0.58	0.54	0.53	0.50
		±0.05	±0.05	±0.05	±0.05	±0.05
	$\langle R^2 \rangle$	0.51	0.53	0.52	0.50	0.52
		±0.05	±0.05	±0.05	±0.05	±0.05
III	$\langle S^2 \rangle$	0.48	0.47	0.53	0.52	0.48
		±0.05	±0.05	±0.05	±0.05	±0.05
	$\langle R^2 \rangle$	0.48	0.46	0.53	0.47	0.46
		±0.05	±0.05	±0.05	±0.05	±0.05

concave, whereas those belonging to the region below the θ point ($\Phi > \Phi_\theta$) appear to be decreasing and convex. Let us draw the horizontal segments AB connecting the points of the curves that correspond to the two different values of the interaction parameter Φ_A and Φ_B, the differences $\Phi_A - \Phi_\theta$ and $\Phi_B - \Phi_\theta$ being of the same sign. We may then define the estimate of the value of the crossover exponent φ_t as:

$$\tilde{\varphi}_t(N_A, \Phi_A, \Phi_B) = \frac{1}{\ln(N_B/N_A)} \ln\left(\frac{\Phi_A - \Phi_\theta}{\Phi_B - \Phi_\theta}\right) \qquad (41)$$

where N_A and N_B are the coordinates of the points A and B. If equation (20) were exact, the length of the segment AB would not depend on its position (which is determined by N_A) and the ratio $\tilde{\varphi}_t$ would be exactly equal to φ_t. However, the obtained data always yield a monotonic increase of the length of the segment AB when N_A is increasing. In some cases this increase even attains 50% of the initial length, giving evidence of the existence of large corrections to scaling in equation (20). Hence, it is clear that in order to obtain the true value of φ_t we should extrapolate the values of $\ln(N_B/N_A)$ to $N_A \to \infty$, which, unfortunately, has not been done in refs. 3, 4 and 33. If the corrections to scaling are analytical, the correction term decreases as $1/N_A$, and, hence, in order to perform linear extrapolation, we have plotted the values $|A_iB_i| = \ln(N_{B_i}/N_{A_i})$, obtained from *Figure 12*, against $\lambda_A = 1/N_A$ (see *Figure 13*). As a result, we obtain the set of limiting values of the segment length $|AB|_i =$

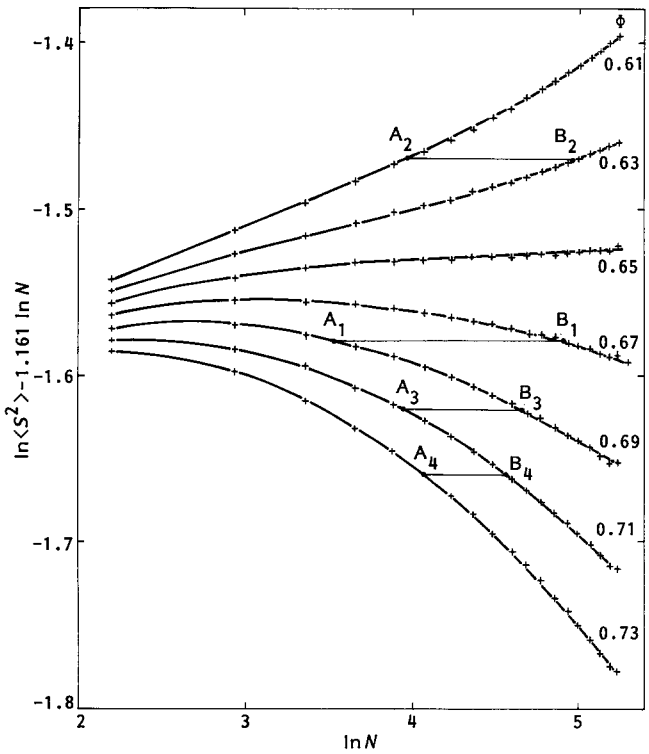

Figure 12 The dependences of $\ln(\langle S^2\rangle/N^{2\nu_t})$ on $\ln N$ for the 1PSAWS model at different values of Φ, shown on the plot. See explanations in the text

$\lim_{N_{A_i}\to\infty}|A_iB_i|$, which corresponds to different pairs of values (Φ_{A_i}, Φ_{B_i}). Choosing the value Φ_θ so that the estimates $\tilde{\varphi}_i = \ln[(\Phi_{A_i}-\Phi_\theta)/(\Phi_{B_i}-\Phi_\theta)]/|AB|_i$ for all pairs (Φ_{A_i}, Φ_{B_i}) are close to each other, we obtain the final approximation of the crossover exponent (see *Table 4*). Naturally, this method also yields large errors because the extrapolation procedure is not well determined. As a result, we can affirm with high degree of reliability that if the universal value of the exponent φ_t exists it must be confined within the interval between the values 0.42 and 0.6. The value $\varphi_+ = 3/7$, obtained in ref. 2, lies near the boundary of the confidence interval, and thus cannot be ruled out.

Let us now discuss the question about the plots of the scaling function $f_X(y)$ (see equation (20)). As has been mentioned in ref. 54, these plots have the best matching of points, corresponding to different values of τ and N throughout the vast interval of τ at some values of critical exponents, which by no means are exact. If one takes the exact values, the matching is good only within a narrow temperature neighbourhood of the critical point and at large N only. The attempt to match the branches of the scaling function in the broad interval of τ by varying the values of φ_t, ν_t, Φ_θ may lead to artifacts.

Nevertheless, in order to illustrate the correctness of the predictions of the scaling theory as a whole, we have plotted all the obtained data, concerning $\langle S^2\rangle$, for all the models on a single scaling plot of the function $\tilde{f}_S(y) = \ln f_S(y) - \ln f_S(0)$ against $\ln(N^{\varphi_t}|\tau|)$ (see *Figure 14*). For best matching of the branches, we have chosen $2\nu_t = 1.175$, $\varphi_t = 0.6$ and the following values of Φ_θ: 0.65, 0.97 and 0.41 for the square, honeycomb and triangular lattices, respectively. The reduced temperature τ has been defined as:

$$\tau = \begin{cases} -1 + \Phi_\theta/\Phi & \Phi > \Phi_\theta \\ 1 - \Phi/\Phi_\theta & \Phi < \Phi_\theta \end{cases} \qquad (42)$$

This definition may be useful because, being defined by (42), τ remains a small quantity, whose absolute value is less than unity.Finally, the constant $\ln f_S(0)$ has been assumed to be -1.58, -1.39 and -1.72 for the square, honeycomb and triangular lattices, respectively. The position of the straight line 2 has been determined for the ground state, which is attained when $\Phi = \infty$, i.e. when $\tau = -1$, and for which, as is easy to calculate, the quantity $\langle S^2\rangle/N$ is equal to 1/6, 5/36 and 5/24 for square, honeycomb and triangular lattices. It appears that the quantity:

$$\ln(\langle S^2\rangle/N)|_{\tau=-1} - \ln f_S(0)$$

is equal to approximately 0.2 for all the models. Hence, the position of the straight line 2 is also similar for all the models.

Summarizing, we can conclude that the data of *Figure 14* match well with two branches of the same scaling function. This matching confirms the universality of the behaviour of the scaling function $f_S(y)$ for different lattices

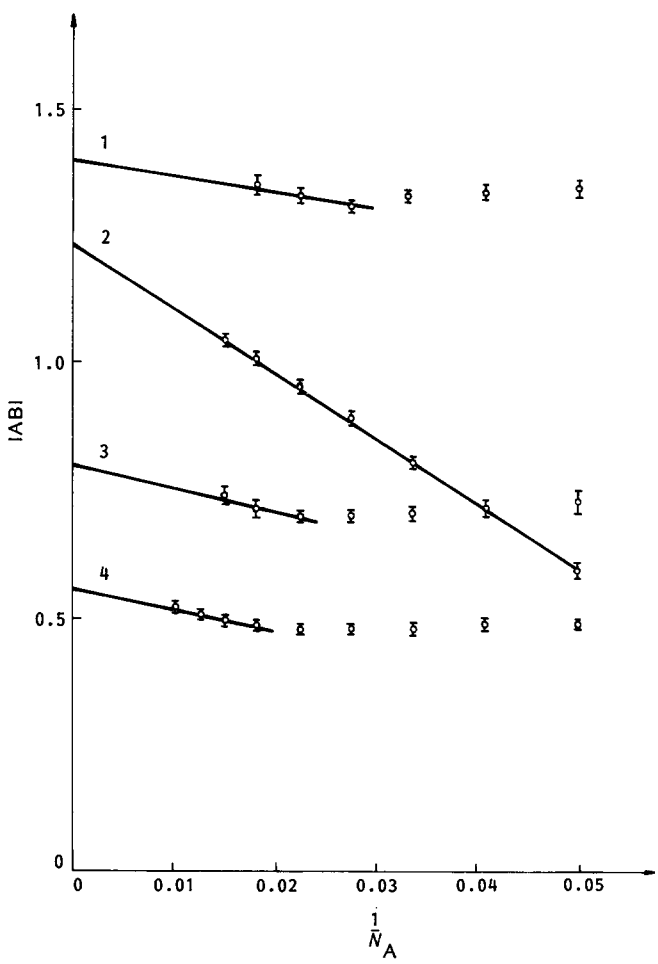

Figure 13 The length of the segment $|A_iB_i|$ vs. $1/N$, according to the data of *Figure 12* for the 1PSAWS model. The series of points denoted by numbers $i = 1, 2, 3, 4$ correspond to the pairs of values of (Φ_{A_i}, Φ_{B_i}) on *Figure 12*: for $i = 1$ (0.69, 0.67), for $i = 2$ (0.63, 0.61), for $i = 3$ (0.71, 0.69) and for $i = 4$ (0.71, 0.73). The extrapolation of $|A_iB_i|$ yields $|AB|_1 = 1.40$, $|AB|_2 = 1.24$, $|AB|_3 = 0.80$, $|AB|_4 = 0.55$. Choosing $\Phi_\theta = 0.652$, we attain $\tilde{\varphi}_1 = 0.534$, $\tilde{\varphi}_2 = 0.521$, $\tilde{\varphi}_3 = 0.529$, $\tilde{\varphi}_4 = 0.537$; hence we may assume $\varphi_t = 0.53$ (see *Table 4*)

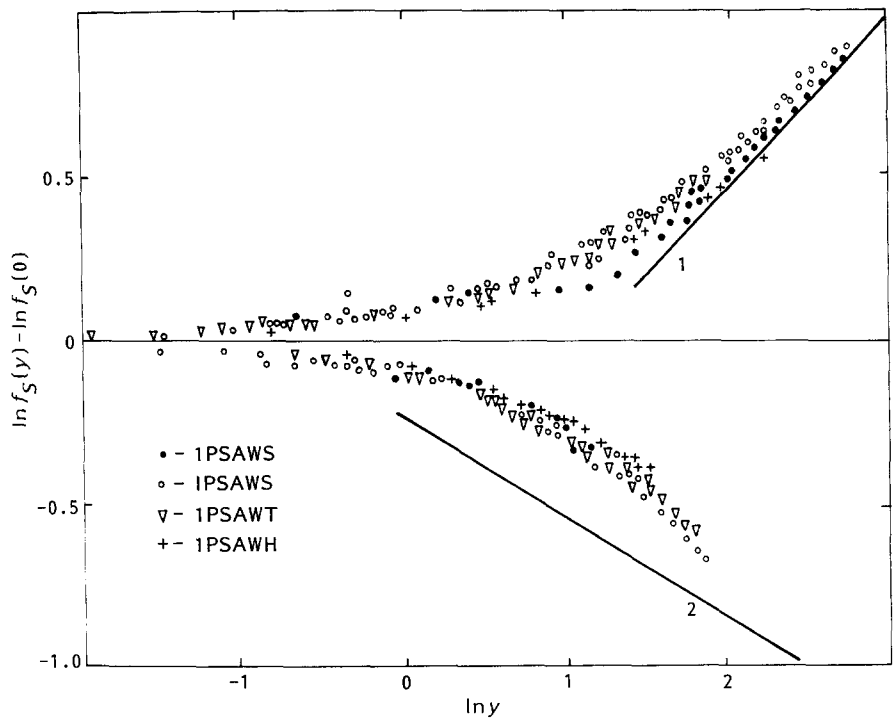

Figure 14 The scaling plot of the function $\ln[f_S(y)/f_S(0)]$ vs. $\ln y = \ln(N^{\varphi_t}|\tau|)$ (see equation (20)) constructed simultaneously for different models with the proper values of parameters of construction. (See explanation in the text.) The slopes of lines 1 and 2 are equal to $\mu_+ = 0.54$ and $\mu_- = -0.29$, respectively (see equations (22) and (23))

and, as a result, the general concept of the θ point as a tricritical point. When an attempt is made to construct that plot with the values $\nu_t = 4/7$, $\varphi_t = 1/2$, the matching is good only within the narrow region $|\tau| < 0.1$, $N \geqslant 150$, but this by no means gives no evidence of the erroneousness of these values.

DISCUSSION OF THE RESULTS

As has been proposed in the recent discussion[8–11,27], the coil–globule transitions in different models of two-dimensional polymers may belong to different universality classes, depending on the type of interaction and lattice. In the present paper we have studied five different models of a macromolecule in a solvent, three of which can be reduced to the traditional model of the self-avoiding walk (SAW) on square, honeycomb and triangular lattices, and the other two are non-traditional models, which cannot be reduced to SAW with nearest-neighbour interactions, but nevertheless can be regarded as models of a macromolecule in a solvent with complicated non-local interactions of monomers. The main and the most important conclusion of our work is, in our opinion, the conclusion that the exponent ν_t is universal for all five models. Its numerical values for all the models are coincident within the range of statistical error with the exact value $\nu_t = 4/7$, predicted in refs. 1 and 2. Probably, the exponent ν_t is the most universal of all the exponents that describe the coil–globule transition, because ν_t is connected with the most important geometrical property of a system, which is its fractal dimensionality, and, thus, characterizes not only the whole macromolecule itself, but any of its sufficiently long parts as well.

The model of an infinitely prolonging self-avoiding walk on a square lattice (IPSAWS) can be regarded as a model of the initial part of a very long macromolecule in a solvent, whose fractal dimensionality is the same as of the whole macromolecule. Apparently, the IPSAWS model has the same critical exponents ν_t and φ_t and the same free energy per monomer as the 1PSAWS model, which can be explained by the fact that one of two halves of any SAW is an infinitely prolonging walk. The exponents γ_t of these two models may differ, but our numerical studies (see *Figure 4*, the section on 'Investigation of the free energy' and Appendix 2) show that the exponents γ_t for these two models also coincide.

Another new model that we have studied is the model of an infinitely growing self-avoiding walk on a square lattice (IGSAWS). This model differs from the IPSAWS model in the absence of the Rosenbluths' factor, which may be regarded as the reciprocal of the Boltzmann factor of some additional effective interaction of nearest and some next-nearest monomers. Therefore, there are serious reasons to assume that these models belong to the same universality class of the coil–globule transition. At $\Phi = 0$ our IGSAWS model becomes equivalent to the IGSAWS model without interaction of monomers, which has been studied in ref 5. As frequently mentioned in the literature[1,5,24], this model can be regarded as a model of a polymer exactly at the θ point. Moreover, being parts of the external perimeters of percolational clusters, the IGSAW on the hexagonal lattice has the same fractal dimensionality $d_h = 7/4$, and the exponent $\nu_t = 4/7$. The introduction of the interaction Φ turns the IGSAW model into the IPSAW model with a complicated total interaction that consists of the obvious attraction or repulsion with parameter Φ and the implicit attraction, which compensates the Rosenbluths' factor and corresponds to θ conditions. Thus, the interaction $-\Phi$ must be regarded as the reduced temperature, or, in other words, the deviation from the θ point. Therefore, we may

suppose that both IGSAWS and IPSAWS models have the same critical exponents ν_t and, probably, the same exponents φ_t and γ_t as well. The exponent γ_t is exactly equal to unity for the IGSAW model, and, therefore, this value may be universal for all the models observed in the present paper. Our numerical data confirm this proposal, yielding for all the models a value of γ_t confined within the interval between 0.98 and 1.08, and a value of φ_t confined within the interval between 0.42 and 0.6. Unfortunately, our data do not allow us to make a final conclusion whether the values γ_t and φ_t of the IGSAW model do or do not coincide with those of the other models. Nevertheless, we can affirm that the value of $\gamma_t = 8/7$ of the model of Duplantier and Saleur[2] differs from the values of γ_t of our models, whereas the value of $\gamma_t = 15/14$ proposed in refs. 6 and 27 may be equal to those of all our models, except, of course, IGSAWS. As to the crossover exponent, our data are not sufficiently accurate to rule out completely the value of $\varphi_t = 3/7$ for our models, as well as to prove the universality of any other value ($\varphi_t = 0.5$, for example) for all the models observed in this paper. However, the general behaviour of all the studied quantities displays universality of rather high degree.

The existence of two different universality classes for the θ point and the θ' point has been confirmed recently[59], where it has also been proposed that a continuous line of critical points exists that connects the standard θ point with the θ' point of Duplantier and Saleur[2]. Along this line the critical exponents are continuously changing from the values obtained in ref. 2 for the θ' point to a value that is close to those obtained in the present paper. The accuracy of our numerical data does not allow us to rule out the possibility of our models belonging to different universality classes, corresponding to neighbouring but different points of this line. Only rigorous renormalization group studies can clear up this question.

REFERENCES

1 Coniglio, A., Jan, N., Majid, I. and Stanley, H. E. *Phys. Rev.* (*B*) 1987, **35**, 3617
2 Duplantier, B. and Saleur, H. *Phys. Rev. Lett.* 1987, **59**, 539
3 Birshtein, T. M., Buldyrev, S. V. and Elyashevitch, A. M. *Polymer* 1985, **26**, 1814
4 Birshtein, T. M., Buldyrev, S. V. and Elyashevitch, A. M. *Vysokomol. Soed.* (*A*) 1986, **28**, 634
5 Kremer, K. and Lyklema, J. W. *J. Phys* (*A*) *Math. Gen.* 1985, **18**, 1515
6 Seno, F. and Stella, A. L. *J. Physique* 1988, **49**, 739
7 Seno, F. and Stella, A. L. *Europhys. Lett.* 1988, **7**, 605
8 Poole, P. H., Coniglio, A., Jan, N. and Stanley, H. E. *Phys. Rev. Lett.* 1989, **60**, 1203
9 Duplantier, B. and Saleur, H. *Phys. Rev. Lett.* 1988, **60**, 1204
10 Seno, F., Stella, A. L. and Vanderzande, C. *Phys. Rev. Lett.* 1988, **61**, 1520
11 Duplantier, B. and Saleur, H. *Phys. Rev. Lett.* 1988, **61**, 1521
12 De Gennes, P. G. *J. Physique Lett.* 1975, **36**, L55
13 Le Guillou, J. C. and Zinn-Justin, J. *J. Physique Lett.* 1985, **46**, L137
14 Nienhuis, B. *Phys. Rev. Lett.* 1982, **49**, 1062
15 Stephen, M. J. *Phys. Lett.* (*A*) 1975, **53**, 363
16 Kholodenko, A. L. and Freed, K. F. *J. Chem. Phys.* 1984, **80**, 900
17 Duplantier, B. *Europhys. Lett.* 1986, **1**, 491
18 Duplantier, B. *J. Chem. Phys.* 1987, **86**, 4233
19 Flory, P. J. 'Principles of Polymer Chemistry', Cornell University Press, Ithaca, NY, 1953, p. 672
20 Birshtein, T. M. and Zhulina, E. B. in 'Matemat. Metody Issled. Polymerov' (in Russian) (Eds I. M. Lifshitz and A. M. Moltchanov), Pushchino, 1982, p. 4
21 Di Marzio, E. A. Macromolecules 1984, **17**, 969
22 Deutch, J. M. and Hentschel, H. G. E. *J. Chem. Phys.* 1986, **85**, 527
23 Khokhlov, A. R. *Polymer* 1981, **22**, 447
24 Weinrib, A. and Trugman, S. A. *Phys. Rev.* (*B*) 1985, **31**, 2993
25 Majid, I., Jan, N., Coniglio, A. and Stanley, H. E. *Phys. Rev. Lett.* 1984, **52**, 1257
26 Jan, N., Coniglio, A. Majid, I. and Stanley, H. E. in 'On Growth and Form—Fractal and Non-fractal Patterns in Physics' (Eds H. E. Stanley and N. Ostrowsky), Reidel, Dordrecht, 1986, p. 273
27 Vanderzande, C. *Phys. Rev.* (*B*) 1988, **38**, 2685
28 Ishinabe, T. *J. Phys.* (*A*) *Math. Gen.* 1985, **18**, 3181
29 Privman, V. *J. Phys.* (*A*) *Math. Gen.* 1986, **19**, 3287
30 Privman, V. and Kurtze, D. A. *Macromolecules* 1986, **19**, 2377
31 Baumgärtner, A. *J. Physique* 1982, **43**, 1407
32 Tobochnik, J., Webman, I., Lebowitz, J. L. and Kalos, M. M. *Macromolecules* 1982, **15**, 549
33 Buldyrev, S. V., Birshtein, T. M. and Elyashevitch, A. M. *Vysokomol. soed.* (*A*) 1988, **30**, 1244
34 Meirovitch, H. and Lim, H. A. *Phys. Rev.* (*A*) 1988, **38**, 1670
35 Bishop, M. and Saltiel, C. J. *J. Chem. Phys.* 1988, **89**, 1719
36 Marqusee, J. A. and Deutch, J. M. *J. Chem. Phys.* 1981, **75**, 5179
37 Jug, G. *J. Phys.* (*A*) *Math. Gen.* 1987, **20**, L503
38 Derrida, B. and Saleur, H. *J. Phys.* (*A*) *Math. Gen.* 1985, **18**, L1075
39 Saleur, H. *J. Stat. Phys.* 1987, **45**, 419
40 Dhar, P. and Vannienus, J. *J. Phys.* (*A*) *Math. Gen.* 1987, **20**, 199
41 Vilanove, R. and Rondelez, F. *Phys. Rev. Lett.* 1980, **45**, 1502
42 Kawaguchi, M., Joshida, A. and Tokahashi, A. *Macromolecules* 1983, **16**, 956
43 Granik, S. *Macromolecules* 1985, **18**, 1597
44 Vilanove, R., Rondelez, F. and Poupinet, D. *Macromolecules* 1988, **21**, 2880
45 Saleur, H. and Duplantier, B. *Phys. Rev. Lett.* 1987, **58**, 2325
46 Hammersley, J. M. and Handscomb, L. C. 'Monte-Carlo Methods', Chapman and Hall, London, 1964, p. 130
47 Hammersley, J. M. and Montron, K. W. *J. R. Stat. Soc.* (*B*) 1954, **16**, 23
48 Rosenbluth, M. N. and Rosenbluth, A. W. *J. Chem. Phys.* 1955, **23**, 356
49 McCrackin, F. L. *J. Res. Nat. Bur. Stand.* (*B*) 1972, **76**, 193
50 McCrackin, F. L., Masur, J. and Guttman, C. M. *Macromolecules* 1973, **6**, 859
51 Hemmer, S. and Hemmer, P. S. *J. Chem. Phys.* 1984, **81**, 584
52 Buldyrev, S. V. and Birshtein, T. M. *Vysokomol. soed.* (*B*) 1988, **30**, 392
53 Birshtein, T. M. and Buldyrev, S. V. *Vysokomol. soed.* (*A*) *1989*, **31**, 104
54 Fähner, M., Keller, W.-U. and Kronmüller, H. *Phys. Rev.* (*B*) 1987, **35**, 3640
55 De Gennes, P. G., 'Scaling Concepts in Polymer Physics', Cornell University Press, Ithaca, NY, 1979, p. 324
56 Eisenriegler, E., Kremer, K. and Binder, K. *J. Chem. Phys.* 1982, **77**, 6296
57 Guttman, A. J. *J. Phys.* (*A*) *Math. Gen.* 1987, **20**, 1939
58 Zamolodchikov, A. B. *Pis. Zh. Eksp. Teor. Fiz.* 1986, **43**, 565
59 Poole, P. H., Coniglio, A., Jan, A. and Stanley, H. E. *Phys. Rev.* (*B*) 1989, **39**, 495
60 Kremer, K. and Lyklema, J. W. *Phys. Rev. Lett.* 1985, **55**, 2091
61 Pietronero, L. *Phys. Rev. Lett.* 1985, **55**, 2025
62 Pelity, L. *J. Physique Lett.* 1984, **45**, 1925
63 Privman, V. *Physica* (*A*) 1985, **123**, 428

APPENDIX 1

On the model of kinetically growing walks (KGW)

One model, regarded to be a model describing a two-dimensional polymer at the θ point was the KGW model, studied for the first time by the Rosenbluths[48] as early as 1955. But it was as late as 1984[25] when this model received its present name. Those authors[25] proposed that the KGW model belonged to the tricritical universality class. However, this hypothesis was not confirmed by further investigations[60–62], and it was proposed that KGW belongs to the universality class of good solvents. The aim of the present study is to confirm

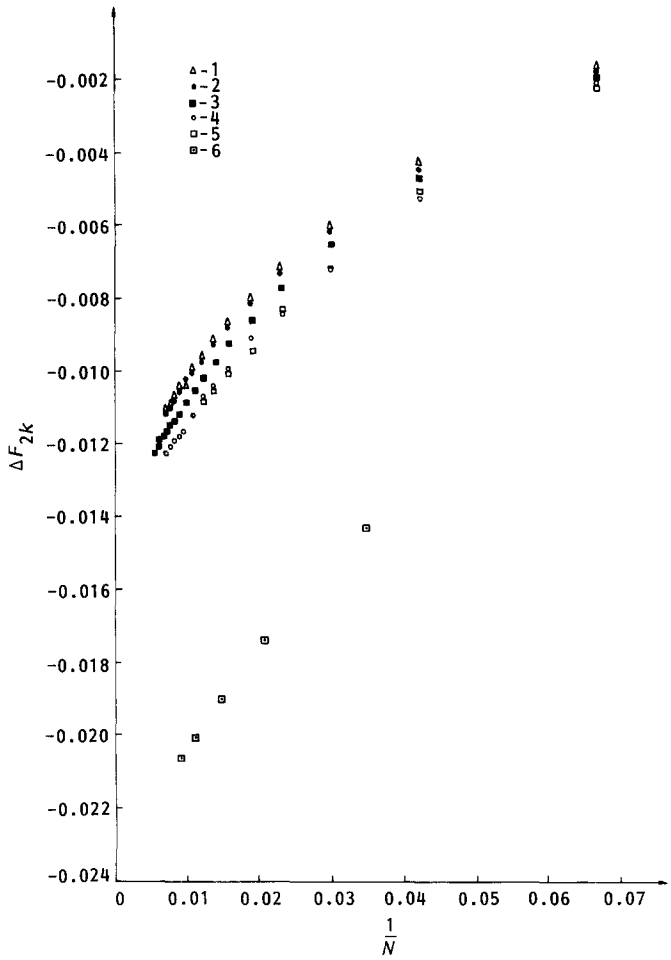

Figure 15 The dependences of ΔF_{2k} on $1/N$ for different models of kinetically growing walks on different lattices, constructed with different values of construction potential Ψ: (1) 1PKGWT, $z=6$, $\Psi=-0.15$; (2) 1PKGWH, $z=3$, $\Psi=0.6$; (3) 1PKGWS, $z=4$, $\Psi=0.3$; (4) 1PKGWS, $z=4$, $\Psi=-0.3$; (5) 1PKGWH, $z=3$, $\Psi=-0.6$; (6) KGWS, $z=4$, $\Psi=0$, data of ref. 51; $k=5$ for (1)–(5), $k=10$ for (6)

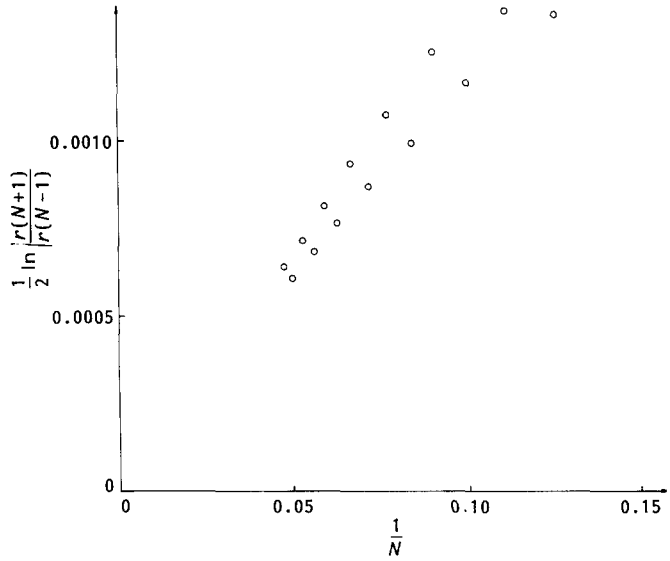

Figure 16 The dependence of $\frac{1}{2}\ln[r(N+1)/r(N-1)]$ on $1/N$ (see Appendix 2)

the latter proposal. The KGW model differs from the standard SAW model in the procedure of averaging of their characteristics. We can obtain the KGW model in the framework of the description in the second section of this work if in equations (9)–(11) we put the Rosenbluths' factor equal to unity, $r_i \equiv 1$, and assume also that $b_i \equiv 1$, $t_{ijk} \equiv 1$, $\Phi=0$, $\Psi=0$. In order to distinguish that averaging from the standard one, we shall mark it by the subscript K for example $\langle R^2\rangle_K$, $\langle Z\rangle_K$. It is clear that, according to equations (9)–(11), taking into account $r_i=1$, $b_i=1$, we shall obtain that:

$$\langle Z(N)\rangle_K = (1/M)\sum_{i=1}^{M} w_i = M(N)/M \qquad (43)$$

i.e. the partition function of the KGW model is equal to the probability of construction of the walk of length N without self-intersections in the framework of the Rosenbluths' method.

As clearly follows from equations (9)–(11), the KGW model on the hexagonal lattice is equivalent to the SAW model if one puts its interaction parameter $\Phi=\ln 2$. This value is sufficiently less than its value $\Phi_\theta=1.02$, which corresponds to the θ point, according to our numerical data. Therefore, the KGW model on the honeycomb lattice belongs to the region of good solvents and the

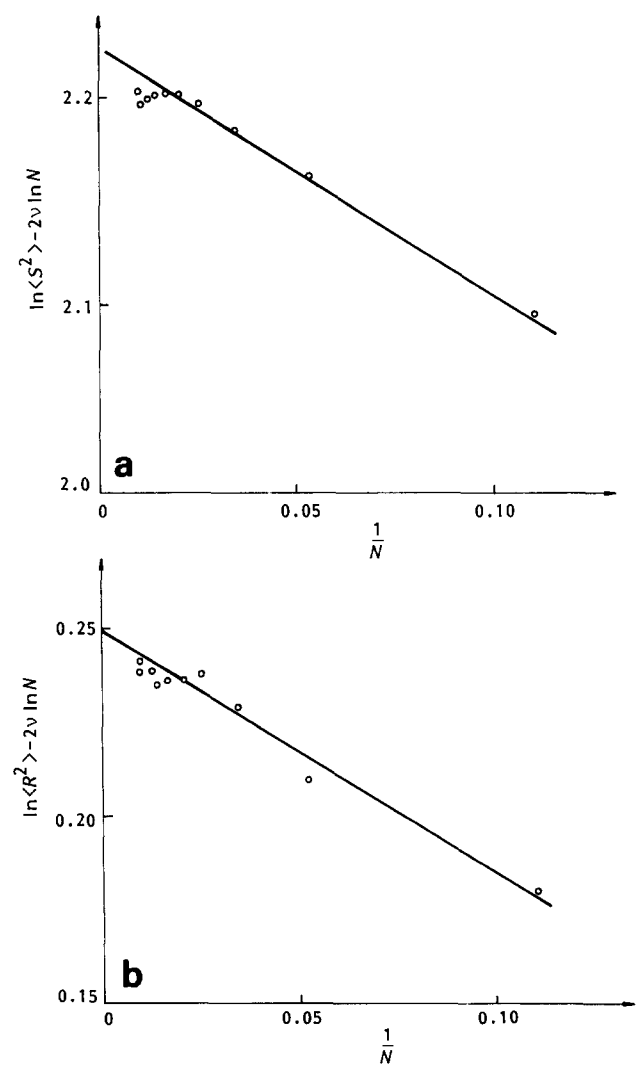

Figure 17 The dependences of corrections to scaling on $1/N$ for the 1PSAWS model at $\Phi=0$: (a) $\ln\langle S^2\rangle - 2\nu\ln N$, (b) $\ln\langle R^2\rangle - 2\nu\ln N$, $\nu=\frac{3}{4}$

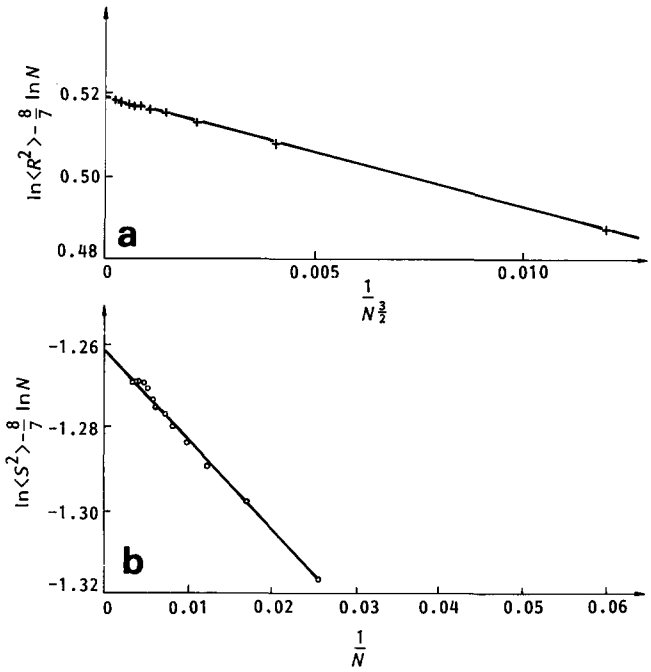

Figure 18 The dependences of corrections to scaling for the IGSAWS model at $\Phi=0$: (a) $\ln\langle R^2\rangle-(8/7)\ln N$ vs. $1/N^{3/2}$, and (b) $\ln\langle S^2\rangle-(8/7)\ln N$ vs. $1/N$

asymptotic behaviour of the value $\langle R^2\rangle_K$ must undergo a crossover from $N^{2\nu_t}$ at small N to $N^{2\nu}$ at large N. The Rosenbluths' estimate[48] $N^{1.26}$ at $N=100$ and the estimate[25] $N^{1.33}$ at $N=300$ belong to this crossover region.

The value $\langle Z(N)\rangle_K$ was studied in ref. 51, where SAWs on the square lattice were constructed by the Rosenbluths' method and the probability of termination of the walk at the Nth step was calculated:

$$\Delta Z(N)=\langle Z(N+1)\rangle_K-\langle Z(N)\rangle_K$$

and the mean length of KGW until its termination was estimated as:

$$\bar{N}=\sum_{N=1}^{\infty} N\Delta Z(N)\approx 71 \tag{44}$$

Unfortunately, the asymptote of the quantity $\Delta Z(N)$ at large N was calculated erroneously in ref. 51, and because of that it was not determined there that the KGW model belongs to the universality class of good solvents. We have analysed the numerical data of that work[51] with the help of equation (14), which has been written, according to the analogy with equations (28)–(31), for the region of good solvents. *Figure 15*, which is analogous to *Figure 4*, shows the dependence of the quantity:

$$\Delta F_{2k}\left(\frac{1}{N}\right)=\frac{1}{2k}\ln\left(\frac{\langle Z(N+k)\rangle_K}{\langle Z(N-k)\rangle_K}\right) \tag{45}$$

on $\lambda=1/N$. Beside that, we have constructed analogous plots according to our own numerical data for the quantity $M(N)/M$, obtained for the 1PSAW model on different lattices and at different values of construction potential Ψ (see also *Figure 15*). It is clear that when r_i in equation (11) is equal to unity, all these models become KGW models of different types, which we have called models of one-prolonging kinetically growing walks (1PKGW). These models apparently belong to the same universality class as the common KGW model. Linear extrapolation of the quantity $\Delta F_{2k}(\lambda)$ up to $\lambda\to 0$ yields:

$$\Delta F_{2k}(\lambda)=(\gamma_k-1)\lambda+\ln\zeta \tag{46}$$

where $\zeta=\zeta_0$ for KGW and $\zeta=\zeta_1$ for 1PKGW. It can be seen that the values of γ_k for the KGW and 1PKGW models are very close to each other and do not depend on the type of lattice and the value of $\Psi(\gamma_k=1.35\pm0.05)$. At the same time, the quantity ζ differs considerably in the KGW and 1PKGW models and depends on the type of lattice and the value of Ψ.

The obtained result gives convincing evidence that the KGW and 1PKGW models belong to the universality class of good solvents, for which $\gamma_k=43/32$ (ref. 14). Thus, the question of the KGW model can be excluded from the agenda.

APPENDIX 2

Determination of the exponent γ_k for IPSAWS from the data of the exact enumeration

The numbers $L_\infty(N)$ of all the infinitely prolonging walks of length N on the square lattice are calculated in ref. 5 up to the value $N=21$. Using the data on the numbers $L(N)$ of all SAW of length N (see ref. 57), we have studied the asymptotic behaviour of the ratio $r(N)=L(N)/L_\infty(N)$ when $N\to\infty$.

Since it is known that the asymptote of $L(N)$ has the form:

$$L(N)\sim\tilde{z}_S^N N^{\gamma-1} \tag{47}$$

it is reasonable to assume that the asymptotic behaviour of $L_\infty(N)$ has the form:

$$L_\infty(N)\sim\tilde{z}_\infty^N N^{\gamma_\infty-1} \tag{48}$$

Therefore, the ratio of these quantities behaves as:

$$r(N)=(\tilde{z}_S/\tilde{z}_\infty)^N N^{\gamma-\gamma_\infty} \tag{49}$$

Figure 16 shows the dependences of the quantity:

$$\Delta F_2(1/N)=\tfrac{1}{2}\ln[r(N+1)/r(N-1)] \tag{50}$$

on $\lambda=1/N$ for even and odd N. It can be observed that the extrapolated straight lines for both branches of the dependence $\Delta F_2(\lambda)$ intersect the ordinate in the region of negative values, i.e. $\Delta F_2(0)\leqslant 0$ or $\tilde{z}_S-\tilde{z}_\infty\leqslant 0$. This difference cannot be negative because in the opposite case the ratio $r(N)$ would tend to zero, which is impossible. Therefore, we must conclude that $\tilde{z}_S=\tilde{z}_\infty$, and the slopes of the dependences $\Delta F_2(\lambda)$, decrease when $\lambda\to 0$. Hence, the quantity $\Delta\gamma=\gamma-\gamma_\infty$ must be less than the effective values of the slopes of these dependences at the least attained values of λ, i.e. $\Delta\gamma<0.012$. Therefore, it is possible that γ_∞ is exactly equal to γ. This conclusion is also confirmed by our approximate Monte-Carlo calculations here (see *Figure 5*). The equality of the free-energy exponents in the region of good solvents naturally suggests the hypothesis of the equality of the tricritical exponents for these two models, which is also in good agreement with our numerical data.

APPENDIX 3

Investigation of corrections to scaling

Determination of corrections to scaling is always a

difficult problem. Even in the classical case of SAW without attraction, when the value of critical exponent $\nu = 3/4$ is exactly known, the results of determination of the exponent Δ in the formula:

$$\langle R^2 \rangle \sim a^2 N^{2\nu}(1 - bN^{-\Delta}) \tag{51}$$

by means of numerical experiments are spread over a wide interval from 0.65 (ref. 63) to 1.5, according to the theory of Nienhuis[14]. The majority of numerical experiments do not find the corrections greater than analytical ones ($\Delta = 1$), which correspond to the end effects in lattice models.

Our numerical experiments show (see *Figure 17*) that the analytical term $\Delta = 1$ prevails in equation (51) for the 1PSAWS model ($\Phi = 0$). For the IGSAWS model ($\Phi = 0$), assuming that $\nu_t = 4/7$, we obtain that $\Delta = 1.5$ for $\langle R^2 \rangle$ and that the analytical term is still prevailing for $\langle S^2 \rangle$ (see *Figure 18*).